Title
The Effect of Titanium Implants on the Peripheral Circadian Rhythm of Bone

Author
McCarville, Kirstin Ty

Publication Date
2013

Peer reviewed|Thesis/dissertation

UNIVERSITY OF CALIFORNIA

Los Angeles

The Effect of Titanium Implants on the Peripheral Circadian Rhythm of Bone

A thesis submitted in partial satisfaction

of the requirements for the degree Master of Science

in Oral Biology

by

Kirstin Ty McCarville

2013

ABSTRACT OF THESIS

The Effect of Titanium Implants on Peripheral Circadian Rhythm in Bone

By

Kirstin Ty McCarville

Master of Science in Oral Biology

University of California, Los Angeles, 2013

Professor Ichiro Nishimura, Chair

BACKGROUND: Endosseous implant osseointegration has been primarily studied by a wound healing-model. The molecular pathway of endosseous implant osseointegrations is not known. Previous animal studies have shown vitamin D insufficiency impairs the establishment of implant osseointegration. Recent microarray data found an interesting connection between vitamin D receptor and circadian rhythm genes using a vitamin D insufficient animal model (implant failure model). Per1 is one of the circadian genes and has widely been used as a molecular marker of circadian rhythm. Previous experiments with forskolin-synchronized expression of Per1 in bone marrow mesenchymal stromal cells (BMSCs) in vitro showed vitamin D supplementation significantly and dose dependently increased the baseline expression of

Per1::luc, but preserved the circadian rhythm. We have thus postulated that the circadian rhythm of BMSCs may be influenced by titanium dental implant.

OBJECTIVES: To determine the effect of titanium implant substrates with different surface characteristics on BMSCs peripheral circadian rhythm.

METHODS: In this study, a series of in vitro studies were designed to characterize the peripheral circadian rhythm of BMSCs harvested from Per1::luc transgenic Wistar rats. Per1 transgenic rats genomic locus of Per1 allele were modified by inserting a beetle luciferase reporter gene (Per1::luc). The peripheral circadian rhythms over a 24-hour period were monitored by the real time activation of luciferase-mediated bioluminescence. Lumicycle was the instrument used to record the luciferase activity (Per1 expression) every ten minutes over five days. Data were evaluated both in the raw form (photons/second) Per1 gene expression and baseline subtracted data. The baseline subtracted data provides the peaks, troughs and periods of the BMSCs peripheral circadian rhythm over 5 days. The first experiments were completed on plastic cell culture dishes with and without vitamin D supplementation.

In the second project, two titanium substrates with polished (smooth) surface or complex (rough) surface with blasted, acid etched and discrete HA crystalline deposition were characterized. Surface topography: Sa (average surface roughness) and Sdr (hybrid parameter that presents information about the number and height of peaks of a given surface) were determined by a 3D surface profilometry. To ensure BMSC survival and proper attachment a WST-1 assay was completed. To determine the level of osteoblast differentiation capabilities of BMSCs on all three surfaces (plastic, smooth and rough) a calcium mineralization assay was preformed.

In the third project, BMSC peripheral circadian rhythm studies were then executed on smooth and rough titanium surfaces with and without vitamin D supplementation. This study was accomplished using Per1:;luc BMSCs and Lumicyle.

In the forth project, Taqman- based quantitative reverse transcription polymerase chain reaction (RT-PCR) was used to validate gene expression of 6 circadian rhythm-related molecules (Per1, Per2, Id2, Bmal1, Clock, and NPas2).

RESULTS: Bioluminescent raw measurement of Per1 expression on plastic with and without vitamin D showed that vitamin D increased Per1 expression over days 2, 3 and 4. The baseline subtracted data suggested that vitamin D suppressed the amplitude (peak to trough) but maintained the period.

The WST-1 assay revealed that over 4 days the three different surfaces had a comparable number of viable cells. The calcium assay also suggested that the different substrate surfaces did not have large influence on osteogenic differentiation of BMSCs.

The raw measurement of Per1::luc on titanium implant substrates indicated that the rough titanium surface had a significant reduction in Per1 expression (more than 50%) of photons per second in comparison to the smooth surface. Furthermore, rough titanium with vitamin D had a lower Per1 expression when compared to the rough titanium with no vitamin D. The smooth titanium baseline subtracted data showed a consistent rhythm having developed peaks and troughs. The most dramatic difference was seen in the rough surface baseline subtracted data. The rough surface almost completely eliminated the amplitude and period of the peripheral circadian rhythm.

RT-PCR validated that five of the six circadian rhythm genes were downregulated by the rough titanium surface. The only gene upregulated on rough titanium was NPAS2.

CONCLUSION: Titanium material had a negative effect on Per1 expression and amplitude of BMSCs peripheral circadian rhythm. Osseointegration pathway is unknown, however, the peripheral circadian rhythm of BMSCs may play a role in the establishment of implant-bone integration. NPAS2 was found to be highly expressed with the rough titanium substrate. Although speculative, the modulation of peripheral circadian rhythm may lead to successful osseointegration.

The thesis of Kirstin Ty McCarville is approved.

Tara L. Aghaloo

Christopher S. Colwell

Neal R. Garrett

Ichiro Nishimura, Committee Chair

University of California, Los Angeles

2013

TABLE OF CONTENTS

LIST OF FIGURES AND TABLES

PART I: *Per1::luc* Gene Expression and Vitamin D

Introduction

Osseointegration and Circadian Rhythm

Dental implant is a highly successful treatment modality and osseointegration is achieved at high rates. However, there are several vitamin D deficient animal models established by Kelly et al., Dvorak et al. and Wu et al. ,, (3,29,30) which are consistently associated with the decreased osseointegration. Kelly et al. demonstrated a decreased serum 1-25 dihydroxyvitamin D3 by vitamin D deficient diet in rats (3). When compared to the control group, the vitamin D insufficient group showed a significantly lower implant push-in test and on SEM analysis a decreased bone-to-implant contact ratio (3). Kelly et al. concluded vitamin D insufficiency significantly impaired osseointegration in vivo and may play a role in the outcome of implant placement with the increasing prevalence of vitamin D insufficiency in patient populations (3).

A genome-wide microarray study by Mengatto et al. (2011) suggested that 103 genes were modulated by implant placement and vitamin D deficiency. The Kyoto Encyclopedia of Genes and Genomes (KEGG) assigned the highest z-score to the circadian rhythm pathway including neuronal PAS domain 2 (NPAS2), and period homolog 2 (Per2). NPAS2 and cartilage ECM genes were upregulated by implant placement and completely attenuated by vitamin D deficiency. Per2 was upregulated by vitamin D deficiency and showed a complementary expression pattern to the NPAS2 cluster. In conclusion of this study, it appears peripheral circadian rhythms and cartilage extracellular matrix may be involved in the establishment of osseointegration under vitamin D regulation (4).

Central and Peripheral Circadian Rhythm of Clock Genes

The suprachiasmatic nucleus (SCN) located in the hypothalamus has been shown to be a circadian pacemaker in mammals. Removal of the SCN eliminates circadian rhythm patterns of behavioral activity, endocrine output, and many biological processes throughout the organism. Transplantation of SCN tissue into SCN-lesioned rats restores rhythmicity. The SCN of mammals contains a collection of cell-autonomous oscillators that are coupled to each other to form the complete SCN pacemaker that is responsible for setting the phase and period of biological rhythms throughout the organism. Unique to pacemaker SCN, it receives photic input through the retino-hypothalmic tract (RHT), which is required for the entrainment of mammalian circadian rhythms to light dark cycles (5).

The mammalian intracellular circadian oscillator is comprised of both negative and positive elements. Period homologues 1 and 2 (Per1 and Per2) and cryptochrome 1 and 2 (Cry1 and Cry2) are negative elements with CLOCK and BMAL1 as positive acting proteins (Figure 1) (5). At the cell level, circadian rhythms are driven by this self-regulatory interaction of clock genes and their proteins. The heterodimer of the proteins CLOCK:BMAL-1 binds to the E-box elements (CACGTG/T) at the promoter region of Per1-2 and Cry1-2, inducing their transcription. Conversely, Per1-2 and Cry1-2 proteins, by interacting with the CLOCK:BMAL-1 heterodimer operate as negative regulators inhibiting their own transcription (6).

The expression and rhythmic regulation of these clock genes is not unique to the SCN but the same clock genes are widely distributed among many peripheral cells and tissues, including the liver, endocrine tissues, the heart and the skeletal muscles. Forskalin or corticosteroid treatment of fibroblast cell lines can induce stable rhythms of core clock-gene mRNAs in vitro, indicating peripheral oscillators are similar to the SCN pacemaker in terms of basic molecular organization. There is a significant difference between the SCN and peripheral oscillators as the

SCN oscillators can be entrained by light, which has not been shown in peripheral mammalian tissues. This direct photic input provides a crucial link between the outside world and the internal circadian time-keeping mechanism. The SCN clock-gene rhythms have a more rapid response to light than peripheral oscillators. Peripheral oscillators are phase-delayed by 4-12 hours relative to the circadian rhythm in the SCN. Peripheral oscillators using a transgenic rat model showed cultured non SCN tissues express circadian rhythms of luciferase (Luc) expression that is driven by the Per1 promoter that dampen (show a progressive decrease in amplitude of the rhythm) after several cycles, whereas cultured explants of the SCN continue to cycle for many weeks. Therefore, peripheral oscillators are not as robust as the pacemaker oscillator of the SCN. Mechanisms for intracellular communication are presumably unique to the SCN and necessary for its function in synchronizing rhythms in downstream oscillators. SCN pacemaker functions as the coordinator of peripheral tissues that also have inherent circadian properties (5).

Filipski et al. found persistant twenty-four hour changes in liver and bone marrow cells despite suprachiasmatic nuclei ablation in mice. Transcriptional and cell cycle-related rhythms displayed a near normal pattern 24 hr pattern in the absence of SCN and of circadian rhythms in rest-activity and body temperature. These findings indicate the ability of peripheral circadian oscillators to remain synchronized in the absence of the established central pacemaker. The ability of peripheral oscillators to maintain circadian rhythms in the absence of a central pacemaker has been further demonstrated in cultured fibroblasts and cultured murine bone marrow progenitor cells. Nevertheless, these rhythms tended to fade away unless a stimulations (glucocorticoid, serum shock) or environmental 24-hour cycle (temperature, light) was

introduced after a few days in culture, suggesting the need for a regular resetting of free-running peripheral oscillators in order for their coordination to be maintained (7).

There are only 8 genes that have been identified which can alter or eliminate circadian rhythm function. Per1 is one of those genes, which freely cycles in cells, making it an ideal gene to manipulate to show a gene modification linked to a clear phenotype. Ever since luciferase was introduced in real-time luminescence of gene expression, this method has faithfully monitored the rhythms of these circadian genes in the fly, mouse, rat, fungi, immortalized cell lines driven from the rat, zebrafish and humans. Using this noninvasive assay, real time expression of circadian and circadian output genes can be measured (1).

Luciferases are enzymes that emit light. A diverse group of organisms use luciferase-mediated bioluminescene to startle predators, to attract prey, or mates. The beetle of North American firefly releases green light during the oxidation of its chemical substrate, luciferin. Other organisms, including plants, can express the luciferase *(luc)* gene, which will glow faintly green when supplied with luciferin (2).

Transgenic animals with a DNA construct in which the promoter of the gene is fused to the luciferase reporter gene were made for monitoring the circadian oscillation of the transcription. *Per 1::luc* rats and *Per 1::luc* mice have been examined in circadian rhythm studies. In these transgenic animals, the phase of Per1 transcription rhythm in the suprachiasmatic nucleus (SCN) in vivo matched the rhythm of the luciferase mRNA in vivo, as well as the luminescence rhythm form cultured SCN. This indicates that the luminescence reporter can be used in real-time monitoring of Per1 transcription and the first peak in cultured SCN reflects the pea of in vivo Per1 mRNA rhythm (1). A Per1 gene expression transgenic rat with a luciferase knock-in at the Per1 promoter region annotated by *Per 1::luc* is a useful model

that allows for real time tracking of circadian transcription and subsequent catalysis of beetle luciferin, resulting in light expression (1).

Vitamin D Effect on Peripheral Circadian Rhythm

In Nathaniel Hassan's published thesis titled, *Circadian Gene Networks In Bone Regeneration,* his circadian rhythm studies with *Per1::luc* rat BMSCs, indicate vitamin D plays a more significant role in circadian rhythm *per1::luc* gene activation rather than in the maintenance of the circadian system. Per1 gene expression in the vitamin D group of bone mesenchymal stomal cells (BMSCs) showed a significantly increased raw Per1 expression when compared to the control and alcohol groups over all four days in the Lumicycle. Vitamin D condition also affected the amplitude of the baseline subtracted data, which measures the peak to trough distance in photons per second. Vitamin D did not significantly affect any other parameter, period or half max, of the BMSCs circadian rhythm (9).

Aims

1. **Characterize the peripheral circadian rhythm of bone marrow stromal cells (BMSCs) using Per1::luc gene expression on cell culturing dishes, CellTreat® .**

This study was designed to measure the raw *Per1::luc* gene expression of BMSCs using a bioluminescence assay. Followed by the examination of the baseline subtracted data, which will demonstrate the normal circadian rhythm of BMSCs.

2. **Determine the effect of 1-25 dihydroxyvitamin D3 on Per1::luc bone marrow stromal cells (BMSCs) peripheral circadian rhythm.**

This study was designed to measure the raw *Per1::luc* gene expression of BMSCs with and with out 1-25 dihydroxyvitamin D3, using a bioluminescence assay. Followed by the

examination of the baseline subtracted data, which will demonstrate a change in the circadian rhythm of BMSCs.

Methods and Materials

BMSC Harvest and Seeding

Two 10 week old male Per1::luc transgenic Wistar rats were obtained from the UCLA Hillblom Islet Research Center for bone marrow sample harvest. Michael Menaker from the University of Virginia originally supplied the rats to the Hillblom Islet Research Center. The partial sequence cloning vector which placed two luciferace sequences at either end of the *Per1* promoter beginning with the Luc F sequence and ending with the Luc R sequence (10). The Luc F sequence consisted of the sequence 5' – CGCCAAAAACATAAAGAAAGGC-3' where as the Luc R sequence was 5'-TGTCCCTATCGAAGGACTCTGG-3'(10). The *Per1* gene also had an estimated number of 40 copies of the luciferase gene. Both rats were euthanized using the strict UCLA Division of Laboratory Animal Medicine (DLAM) guidelines at the Hillblom Islet Research Center and transported to the Weintraub Center in a covered sealed container with ice. The bone marrow was harvested within 1 hour of rats' termination.

The left and right femurs were removed from both rats and placed into two separate 85mm dishes, each with 10ml phosphate buffer (PBS) and 0.1ml penicillin strep antibiotic (PS). The metaphyses at each end of the femur were clipped and the bone marrow was flushed using a 20 gauge syringe containing 10ml DMEM, 10% FBS (fetal bovine serum), 1%PS solution into a 50ml test tubes. This procedure was completed for the left and right femurs of each rat. The 10ml DMEM, 10%FBS, 1%PS was mixed with a pipette until all bone marrow was dissolved into the solution. The 20ml bone marrow from each rat was plated onto two 85 mm cell-culturing dishes (10ml each plate) and placed in the incubator at 5.0 O2 and 37° F. After two

days the culture medium of each dish was removed and washed two times with 10ml PBS before placing 10ml of cell culturing media (alpha MEM, 10% FBS, 1% PS) in each dish. Cell culturing media consisted of 445ml of alpha MEM, 50 ml of FBS (10%), and 5ml of penicillin strep antibiotic (1%). 85mm cells were washed with 10ml PBS and media replaced with 10ml of alpha MEM, 10% FBS, 1%PS every two days until dishes reached 100% confluent. On day four both dishes had reached 100% confluent and were passaged from P0 to P1.

Cell Passage

Cell passage protocol was completed as follows each time a cell-culturing dish reached confluency. All cell washings and passages during the multiple experiments took place under a hood. Cell culturing media consisted of 445ml of alpha MEM, 50 ml of FBS (10%), and 5ml of penicillin strep antibiotic (1%). 0.25% trypsin, alpha MEM (10% FBS, 1% PS,) and PBS were heated in a 35°C water bath for 15 minutes. Each 85 mm dish medium was suctioned, washed with 10ml of PBS and suctioned. 3ml of 0.25% trypsin was placed onto the 85mm dishes and placed in the incubator (5% CO2 and 37°C) for 3 minutes. Three minutes is a sufficient period of time and trypsin concentrations for most cells to detach from the dish. The dishes were removed from the incubator and 3ml of alpha MEM, 10% FBS, 1% PS was added to the 3ml of 0.25% trypsin solution. Alpha MEM deactivates the trypsin to allow for proper cell attachment. The alpha MEM and trypsin solution was mixed up and down with a pipette to collect as many cells as possible to be transferred into a 15 ml test tube. The 6ml cell solution was placed in the centrifuge at 1000 rpm for 5 minutes with a balancing 6ml test tube. The 6ml supernatant was suctioned leaving the pellet of cells behind in the pipette. The pellet was then re-suspended in 10ml of alpha MEM, 10% FBS, 1%PS. 5ml of the cell solution was placed on each 85mm dish with 5 ml of alpha MEM, 10% FBS, 1% PS added for a total of 10ml solution. Both dishes were

placed back into the incubator and labeled as P1. The 85mm dishes were washed every two days with 10ml of PBS followed by placing 10 ml of alpha MEM, 10%FBS, 1% PS until dishes were 100% confluent which was determined by examining dishes under a phase control 10X microscope.

Cell Plating for Experiment 1: Plastic vs. Plastic with Vitamin D

All experiments done with the *Per1:luc* BMSCs were completed with cells between passage 3 and passage 5. Passage 3 *Per1::luc* BMSCs were used for the plastic surface compared to plastic surface with vitamin D lumicycle loading. Lumicycle protocol was as follows. As described in the paragraph above, cells were washed with PBS, trypsin was used to detach the cells, alpha MEM cell culturing solution was added to trypsin and cells were spun down in the centrifuge. After the cell pellet was re-suspended with 10ml of alpha MEM, 10% FBS, 1% PS, the cell density of this solution was calculated by placing 10µl onto a hemacytometer and the cells were counted in each of the four quadrants of the stage under a phase contrast microscope at 10X magnification. The cell number of each quadrant was added and divided by four. The average number of cells was multiplied by 100,000 to obtain the cell density in cells per milliliter. Since the cells were to be seeded at 20,000 per cm2 on 35mm plates, a total of 192,422.55 was divided by the established cell density to obtain the seeding density in millimeters. The seeding density was then converted to microliters for use of the appropriate pipette. Each 35mm CellTreat® dish (eight total) received the same seeding volume of cell solution in addition to 2ml of alpha MEM, 10% FBS, 1% PS and were placed in the incubator at 37° C and 5% CO2. The eight 35mm plastic dishes with BMSC cells, were allowed to grow four days with a media change after the first two days.

Recording media for the Lumicycle must not contain phenol red as red reduces the light signal penetration. F12 (with no phenol red) was used to replace the alpha MEM in the cell culturing recording media. F12 media with HEPES buffer helps to accommodate the carbon dioxide lacking environment of the Lumicycle. 445ml of F12, 50ml of FBS (10%), and 5ml of Penicillin strep (1%) was used to fabricate the Lumicycle recording media (1).

On the fourth day, the eight dishes were suctioned and washed with 2ml of PBS. 20µl 10nM forskolin was placed in 30ml in F12, 10% FBS and 1% PS. The eight dishes were overlayed with 2ml of forskolin/F12 solution for two hours in the incubator at 37°C and 5% CO2. Forskolin induces stable rhythms or resets the cells peripheral circadian rhythm so all cells are synchronized (5).

The lumicycle recording media was prepared (during the two hour waiting period of forskalin). The lumicycle recording media contained 30ml of F12 10%FBS, 1% PS and 30µl of luciferin. The vitamin D lumicycle recording media consisted of 30 ml F12 10% FBS, 1% PS, 30µl of 1nM vitamin D and 30µl of luciferin. Exactly two hours after the forskolin/F12 solution was placed, the eight dishes were washed with 2ml of PBS. Four CellTreat® dishes received 2ml each of the recording media without vitamin D and the other four CellTreat® dishes received the 2ml each of the special vitamin D recording media. The eight 35mm dishes were grease sealed inside the rim and the outside lip of the cell-culturing dish. The grease used to seal the culturing plates is Corning's high-pressure vacuum grease. Grease sealing is necessary to preserve the cell media so the media does not evaporate during the course of the seven-day experiment (1).

The eight dishes containing P3 BMSCs *Per1::luc*, were transported to the Lumicycle in aluminum foil, concealed from light until dishes were loaded in the Lumicycle. The Lumicycle

is a bioluminescence assay that measures the real time activation of luciferase. It is equipped with four photon counting photomultiplier tubes, each selected for low dark counts and high sensitivity in the green portion of the spectrum at which luciferase emits light. Readings are taken every ten minutes as photon counts per second and all data is recorded on an attached computer for data processing and analysis. The lumicycle is located in a dark room as the photo sensors are very sensitive to light. Each lumicycle loading requires the dishes to be placed in the lumicycle for seven days with no media change or carbon dioxide access. The temperature of the Lumicycle is kept at 37°C, which is viable for cell culturing.

Lumicycle Data Acquisition and Processing

All raw data was analyzed by comparing the average photon count from each day between days one through four. Period was measured by the peak-to-peak, x-axis, distance in days while amplitude was taken as the trough to peak, y-axis. The period and amplitude measures were compared after performing a baseline subtraction and applying a polynomial fit line of sixteen with a smoothing of eighteen hours. Period and amplitude were compared across the different days and conditions. A standard deviation was also generated followed by t test to determine statistical significance both for the raw and baseline subtracted data (11).

Lumicycle Actimetrics a software program was used to perform the baseline subtraction applied under a polynomial filter of 16 and a smoothing of 18 to produce well-defined peaks and troughs from the raw data. The process of baseline subtraction involves the use of a midline drawn between all peaks and troughs so as to normalize the circadian rhythm. The use of this technique allows for the visualization of well-defined peaks and troughs for definition of a rhythm. The polynomial number allowed for the midline to fit a more sensitively to a sinusoid curves that were circadian in nature. The smoothing allowed for the removal of noise (11).

Results

Raw Per1 expression measures the amount of gene expression through photons per second, which were measured every ten minutes. The Raw Per1 expression (Figure 2) of plastic versus plastic with vitamin D BMSCs showed vitamin D increased Per1 expression in days two, three and four, statistically using an analysis of variance (2x4), there was no difference between no vitamin D and vitamin D, F value 0.43, P value 0.5359. Using the delta method in statistics to compare days one through four of the raw Per 1 expression (Figure 3): plastic vitamin D group sustains Per1 expression. Days two and three maintain positive values with vitamin D. Plastic condition without vitamin D in days three and four have a negative expression or value. Using a T test to compare delta days one through four, there is a significant difference between plastic and plastic with vitamin D (Table 2) for days two, three and four.

Baseline subtracted data normalizes the raw data by fitting a zero line midway between the peaks and troughs. The baseline subtraction data describes the peripheral rhythm of the BMSCs through peaks and troughs. Typically the parameters that are measured are amplitude and period. Amplitude is the measurement from peak to trough distance over days (horizontal axis) and photons per second for the vertical axis. Period is the measurement from peak to peak, horizontal axis in days and vertical axis in photons per second. The baseline subtracted data (Figure 4) shows both the amplitude and period for the plastic and the plastic with vitamin D peripheral circadian rhythm. The plastic vitamin D group suppresses the amplitude when compared to the plastic group. However, the period is maintained between both the plastic and plastic with vitamin D. The average amplitude of the baseline subtracted data (Figure 5) shows the plastic group to have a higher amplitude while the vitamin D decreases the amplitude. Using an 2x3 analysis of variance there was no statistical difference between no vitamin D and vitamin

D, F value 2.4 and P value 0.1723. There was a significant difference between amplitudes 1,2 or 3 (Figure 5) F value 147.62 and P value 0.0001. The average period of the baseline subtracted data (Figure 6) shows that both the plastic and the plastic with vitamin D groups maintain nearly the same period over four days.

Conclusion

These results were consistent with the results that were published in Nathanial Hassan thesis (9). Vitamin D significantly increased raw Per1 expression. Vitamin D suppresses the amplitude of the peripheral circadian rhythm but does not affect the period.

Now that a model has been replicated to test the peripheral circadian rhythm of *Per1::luc* BMSCs on cell culturing plates with and without vitamin D, my hypothesis can be studied.

Hypothesis

Peripheral circadian rhythm of bone is affected by titanium implants.

PART II: Titanium Surface Profilometry, Cell Viability and Mineralization

Introduction

Implants have revolutionized dentistry in the 21st century. Worldwide implant use is steadily increasing, reaching more than one million dental implantations per year (12). Implant retained prosthetics can benefit all patients: patients missing a single tooth, partially edentulous and edentulous patients, even maxillofacial patients. Implant design, surface topography, surgical guidelines, and bone-grafting capabilities are changing constantly to meet the demands of patients. The demand is for faster osseointegration and healing, excellent esthetics and an expedited restorative phase, “teeth in a day.”

Clinical success of oral implants is related to their early osseoinegration. Geometry and surface topography are crucial for the short and long term success of dental implants. There can

be two types of bone response when an implant is placed in bone a fibrous soft tissue capsule around the implant, which leads to implant failure or a direct bone to implant contact without an intervening connective tissue layer. The second description is what is known as osseointegration and this biological fixation is considered a prerequisite for long-term success of implant-supported prostheses. The rate and quality of osseointegration in titanium implants are related to their surface properties. Surface composition, hydrophilicity and roughness are parameters that may play a role in implant-tissue interaction and osseointegration (12).

Titanium and Surface Roughness

Dental implants are usually made from commercially pure titanium (cpTi) with varying degrees of purity depending on oxygen, carbon and iron content. Titanium alloys are mainly composed of Ti6Al4V (grade 5 titanium alloy) with greater yield strength and fatigue properties than pure titanium (12). Surface chemical composition also affects the hydrophilicity of the surface. Highly hydrophilic surfaces seem more desirable than hydrophobic ones in view of their interactions with biological fluids, cells and tissues (12). There are numerous reports that demonstrate surface roughness of titanium affects the rate of osseointegration and biomechanical fixation. The main clinical indication for using an implant with a rough surface is the poor quality or volume of the host bone to ensure a better bone to implant contact. Surface roughness can be divided into three levels depending on the scale of the features: macro-, micro- and nano-sized topologies (12).

The macro level is defined for topographical features as being in the range of millimeters to tens of microns. This scale is directly related to implant geometry, with threaded screw and macroporous surface treatments giving surface roughness of more than 10μm. Reports have

shown that both early fixation and long-term mechanical stability of the prosthesis can be improved by a high roughness profile compared to smooth surfaces (12).

The microtopographic profile of dental implants is defined for surface roughness in the range of 1-10μm. This range of roughness maximizes the interlocking between mineralized bone and the surface of the implant (12).

Nanometer roughness plays an important role in the absorption of proteins, adhesion of osteoblastic cells and thus the rate of osseointegration (12). There is an experimental problem that when surfaces are altered with different techniques, microroughness will change simultaneously with nanoroughness, making it difficult to analyze the individual contribution of the two modes of roughness separately. Most techniques used to alter surface roughness, independent of the level of resolution, will also result in unavoidable surface chemical alterations (13).

There are various methods, which have been developed in order to create a rough surface and improve osseointegration of titanium implants, plasma spraying, grit blasting, acid etching, anodization, and calcium phosphate coatings (12). Unfortunately, the standards of surface metrology used in published papers today vary so much that any attempt at a systematic review of the importance of surface roughness in bone healing has inevitable shortcomings (13). For example implant used in one experiment may be determined to be rough implants but in another paper call smooth implants.

Wennerberg and Albrektsson offer their knowledge and opinion on the most accurate way to compare implant surfaces (13). It is felt that 3D evaluations are preferable, the average surface roughness over a surface (Sa value) is more important than average roughness. Sa represents information about average height deviations and a given surface area, which provides

more consistent and reliable information that is not influenced by the measurement direction (13). A positive correlation is found between an increasing Sa value and stronger bone integration, at least up to a certain level of roughness (13). The authors prefer the developed surface ratio (Sdr), a measurement that provides information regarding surface enlargement if a given surface is flattened out. Sdr is a hybrid parameter that presents information about the number and the height of peaks of a given surface. Usually data is analyzed from nine or ten different parameters (13). In animal experiments it seems as though a moderately rough surface with a Sa of about 1.5μm and an Sdr of about 50% promotes the strongest bone response (13). Osseointegration per se is not linked to certain defined surface characteristics, since a great number of different surfaces achieve osseointegration (13). However, stronger or weaker bone response could be related to surface phenomena like changes in mircroroughness, physiochemical effects and nanoroughness (13). One conclusion could be reached Nanotite (Biomet 3i), Osseospeed (Astra Tech), SLActive (Straumann) implants, manufactured by three different companies, have one obvious quality in common: they all have stronger bone response than their respective predecessors with changed microtopography, surface chemistry and modified nanoroughness (13).

Aims

1. **Analyze surface characteristics of polished and B+AE DCD titanium surfaces using SCM and profilemetry analysis.**

This study was designed to measure the surface topography of the polished and B+AE DCD titanium surfaces, measuring the Sa (measure of average surface roughness) and Sdr (developed surface area ratio). B+ AE DCD implant surface is treated by blasted, duel acid

etching and received discrete crystalline deposition of HA nanoparticles (Biomet3i, Palm Beach Gardens, FL) (Figure7) (20).

2. **Determine cell viability and mineralization capabilities on polished and B+ AE DCD titanium surfaces.**

A WST-1 Assay was completed to verify cell attachment and vitamin D's impact on cell adhesion using plastic, polished and B+AE DCD surfaces. Finally, a calcium mineralization assay was completed using an osteogenic medium to evaluate Ca deposition on all three different surfaces, which is representative of in vitro bone formation.

SCM and Profilemetry Analysis

Methods and Materials

One 32mm polished titanium disk, and one 32mm B+ AE+DCD titanium disk were sent to Dr. James Kenealy at Biomet 3*i* clinical research department in Palm Beach Gardens, Florida for scanning electron microscopy and surface topography analysis. The SEM analysis was completed at 10μm for the polished titanium and at 10μm and 500nm on the B+ AE DCD titanium. The surface topography analyzed each surface specimen five times at a 310x magnification on a (machine?), each surface specimen was taken from a different location on the titanium disk. Samples were recorded and read in 10mm lengths. Three profilometry values were recorded at each of the five samples: Sa (mean absolute deviation of height), Sq (root mean squared) and Sdr (Standard deviation of height). Each surface area sampled was then represented in a 3-dimensional map.

Results

Figure 8 shows the SCM of the polished titanium at 10um and the B+AE-DCD (rough) at10um and 500nm. Figure 9 describes the surface topography data of the 35mm polished

titanium surface at 310x in values of Sa, Sq and Sdr. Figure 10 describes the surface topography data of the 35mm B+AE DCD (rough) titanium in values Sa, Sq and Sdr. Figure 11 depicts the surface topography in a bar graph comparing Sa, Sq and Sdr values for both surfaces. Table 4 provides a summary of the four most common implant surfaces compared to the polished and rough implant surfaces used in this experiment.

Conclusion

Table 3 compares the surface topography of the four companies which hold the largest implant market share with the addition of the two implant surfaces used in this experiment (13). The Sa, which provides information about a given surface (average roughness over a surface) for the polished surface was 0.259μm which is smoother than the Osseotite surface and had a much less Sdr percentage (0.5186%). Sdr percentage presents the standard deviation of height. The rough titanium surface used in this experiment had a Sa of 2.06μm,which is higher than SLActive implants at 1.75μm and an Sdr of 14%. In animal experiments it seems as though a moderately rough surface with a Sa of 1.5μm and an Sdr of about 50% promotes the strongest bone response (13). In this experiment the polished surface is very smooth and the "rough" surface has a high Sa value but only a 14% Sdr value.

WST-1 Assay

Methods and Materials

WST-1 assay is a colorimetric assay (WST-1 based) for the nonradioactive quantification of cell proliferation, cell viability and cytotoxicity using a 96-well-plate format. BMSCs were prepared exactly as if the cells were being loaded in the Lumicycle protocol was followed as written earlier with a few minor changes. P3 passage cells were plated on three 10mm polished titanium disks, three 10mm B+ AE DCD (rough) titanium disks that were housed in a 46-well

plate and three plastic wells. The cell media was alpha MEM 10%FBS and 1% Penicillin Strep. Cells were plated at 3000 cells cm^2 using hemacytometer. Plates were placed in the incubator 5%CO^2 37°C. Two days later the plates were removed and the cells were washed with 0.5ml PBS and then synchronized using a forskolin overlay for 2 hours. After the two hours, all four plates were washed with 0.5ml PBS. 0.5ml vitamin D recording media was then placed into the nine wells. Plates were grease sealed with Corning's high-pressure grease and placed in an incubator with no CO^2 at 37°C. That same day to simulate the first couple of hours of the BMSCs in the Lumicycle, Day 0 plate was removed and prepared to receive the WST-1 reagent. Cell Proliferation Reagent WST-1 by Roche was used to complete the assay. Directions were followed as specified per Roche WST-1 Assay pdf (17). The culture solution reagent ratio should be 10:1 (.50ml tissue culture medium: 50µl reagent). 50µl of reagent was added to each of the nine wells. The plate was placed in the incubator for 1 hour. The Day 0 plate was removed from the incubator and agitated for one minute. Three 100µl samples were taken from each of the nine wells (3 plastic, 3 polished, 3 rough) and placed in a 96-well plate. There was also a triplicate of 9 wells which served as a control (no cells). The 96-well plate was then read by a plate reader (Synergy H1) looking at absorbance endpoint, at a wavelength of 450. Day 1 plate was prepared with the WST-1 reagent twenty-four hours later, followed by Day 2 plate forty-eight hours later and finally Day 3 plate seventy-two hours later. Each plate was read at the same time of day (within one hour) and the same specifications on the Synergy H1 at an absorbance endpoint, wavelength 450 (17).

Results

As Figure 12 depicts with the WST-1 assay, cell proliferation increased from day 0 to day 1 for all surfaces. Cell proliferation increased on day 2 only in the polished titanium group. On

day 3 all groups decreased in proliferation except the plastic group but were still greater than the cells at baseline day 0. Using a two way analysis of variance there was no main effect comparing the three surfaces, F value 0.85 and P value 0.4720. The importance of this assay was to show that BMSCs do attach and proliferate on all three surfaces over four days. At day four there are still more cells than the initial seeding density on day 0.

Ca Mineralization Assay

Methods and Materials

BMSCs were prepared as if the cells were being loaded in the Lumicycle, protocol was followed as written earlier with a few minor changes. P3 passage cells were plated on three 10mm polished titanium disks, three 10mm B+ AE DCD (rough) titanium disks that were housed in a 46-well plate and three plastic wells. The cell media fabricated was a differentiating media. The differentiating media was comprised of: 1 ml of each Dexamethazone (10^{-8}), Beta Glycerophosphate (10mM), ascorbic acid (50μg/ml) and 97ml of alpha MEM 10%FBS 1%penicillin strep. Cells were plated at 3000 cells cm^2 using hemacytometer. 1ml of differentiating media was placed over each of the nine wells. The 46-well plate was placed in the incubator 5%CO^2 37°C. The differentiating media was changed every three days for twelve days.

On the thirteenth day the calcium mineralization assay prep began by using the Stanbio Laboratory Calcium (CPC) Liquicolor kit. Protocol was followed per CPC Liquicolor kit.

Results

Figure 13 in a bar graph describes the calcium levels in mg/dl for the three surfaces examined. A one-way ANOVA was completed comparing each surface, which had 3 subjects each. The F value was 26.011 and the p value was significant p 0.001. When a post hoc

comparison was completed using a Bonferroni correction analysis with 3 comparisons (3 hypothesis) the corrected p value was .0167. After the Bonferroni correction, there was only a significant difference between the polished titanium and the plastic surface. The other two comparisons were not significant.

Conclusion

The plastic surface had the highest calcium mg/dl, followed by the rough surface and finally, the polished surface. The BMSCs were most differentiated on the plastic surface as having the most calcium deposition.

PART III: *Per1::luc* Gene Expression on Polished and Rough Titanium Surfaces

Aim

1. Measure the peripheral circadian rhythm of bone marrow mesenchymal stromal cells (BMSCs) using *Per1::luc* gene expression in vitro on polished and B+AE DCD titanium surfaces.

Methods and Materials

A raw median measurement of Per1::Luc gene expression of BMSCs with and without 1,25 dihydroxyvitamin D3 will be evaluated using a bioluminescence assay. Followed by the examination of the baseline subtracted data, which will show the circadian rhythm of BMSCs on the different titanium surfaces with and without vitamin D.

BMSC Harvest and Seeding

Two 10 week old male Per1::luc transgenic Wistar rats were obtained from the UCLA Hillblom Islet Research Center for bone marrow sample harvest. Michael Menaker from the University of Virginia originally supplied the rats. The partial sequence-cloning vector which was placed two luciferace sequences at either end of the Per1 promoter beginning with the Luc F

sequence and ending with the Luc R sequence (15). The Luc F sequence consisted of the sequence 5' – CGCCAAAAACATAAAGAAAGGC-3' where as the Luc R sequence was 5'-TGTCCCTATCGAAGGACTCTGG-3' (15). The Per 1 gene also had an estimated number of 40 copies of the luciferase gene. Both rats were euthanized using the strict UCLA Division of Laboratory Animal Medicine (DLAM) guidelines at the Hillblom Islet Research Center and transported to the Weintraub Center in a covered container with ice. The bone marrow was harvested within 1 hour of rats' termination.

The left and right femurs were removed from both rats and placed into two separate 85mm dishes, each with 10ml phosphate buffer (PBS) and 0.1ml penicillin strep antibiotic (PS). The metaphyses at each end of the femur were clipped and the bone marrow was flushed using a 20 gauge syringe containing 10ml DMEM, 10% FBS (fetal bovine serum), 1%PS solution into a 50ml test tubes. This procedure was completed for the left and right femurs of each rat. The 10ml DMEM, 10%FBS, 1%PS was mixed with a pipette until all bone marrow was dissolved into the solution. The 20ml from each rat were then plated onto two 85 mm cell culturing dishes and placed in the incubator at 5.0 CO^2 and 37° F. After two days the supernatant of each dish was removed and washed two times with 10ml PBS before placing 10ml of cell culturing media (alpha MEM, 10% FBS, 1% PS) in each dish. Cells washed with 10ml PBS and media replaced with 10ml of alpha MEM, 10% FBS, 1%PS every two days until dishes were 100% confluent. On day four both dishes had reached 100% confluency and were passaged from P0 to P1.

Cell passage protocol was completed as follows for each passage necessary during the experiment under the hood. 0.25% trypsin, alpha MEM, 10% FBS, 1% PS, and PBS were heated in a 35°C water bath for 15 minutes. Each 85 mm dish supernatant was suctioned, washed with 10ml of PBS and suctioned. 3ml of 0.25% trypsin was placed into the 85mm dishes and placed

in the incubator (5% CO^2 and 37°C) for 3 minutes. Three minutes is a sufficient period of time and trypsin concentrations for most cells to detach from the dish. The dishes were removed from the incubator and 3ml of alpha MEM, 10% FBS, 1% PS was added to the 3ml of 0.25% trypsin solution. Alpha MEM deactivates the trypsin. The alpha MEM and trypsin solution was mixed up and down with a pipette to collect as many cells as possible to be transferred into a 15 ml test tube. The 6ml cell solution was placed in the centrafuge at 1000 rpm for 5 minutes with a balancing 6ml test tube. The 6ml supernatant was suctioned leaving the pellet of cells behind. The pellet was then re-suspended in 10ml of alpha MEM, 10% FBS, 1%PS. 5ml of the cell solution was placed on in each 85mm dish with 5 ml of alpha MEM, 10% FBS, 1% PS added to each dish for a total of 10ml solution. Both dishes were placed back into the incubator. The 85mm dishes were washed every two days with 10ml of PBS followed by placing 10 ml of alpha MEM, 10%FBS, 1% PS until dishes were 100% confluent which was determined by examining dishes under a phase control 10X microscope.

Passage 3 Per1::luc BMSCs were used for the lumicycle loading. Lumicycle protocol was as follows. As described in the paragraph above, cells were washed with PBS, trypsin was used to detach the cells, alpha MEM solution added to trypsin and cells were spun down in the centrifuge. After the cell pellet was re-suspended with 10ml of alpha MEM, 10% FBS, 1% PS, the cell density of this solution was calculated by placing 10μl onto a hemacytometer and the cells were counted in each of the four quadrants of the stage under a phase contrast microscope at 10X magnification. The cell number of each quadrant was added and divided by four. The average number of cells were multiplied by 100,000 to obtain the cell density in cells per ml. Since the cells were to be seeded at 20,000 per cm^2 on 35mm, a total of 192,422.55 was divided by the established cell density to obtain the seeding density in millimeters. The seeding density

was then converted to micro liters for use of the appropriate pipette. The polished titanium 32mm disks (eight total) received the 20,000 per cm^2 seeding density but only had 1.5ml of alpha MEM, 10% FBS and 1% PS cell culturing media per 35mm dish. The B + AE DCD disks were soaked over night in alpha MEM prior to placing the same seeding density due to the hydrophobic nature of the rough titanium surface. Eight B +AE DCD 32mm disks were seeded at the same cell density and had 1.5ml of alpha MEM, 10% FBS and 1% PS placed in each dish. All sixteen 35mm dishes were placed in the incubator at 5% CO^2 and 37°C. The BMSC cells were then allowed to grow four days with a media change after the first two days. On the fourth day, the sixteen dishes were suctioned and washed with 2ml of PBS. 10µl 10nM forskolin was placed in 30ml in F12, 10% FBS and 1% PS. The sixteen dishes were overlaid with 2ml of forskolin F12 solution for two hours in the incubator at 5% CO^2 and 37°C. The lumicycle recording media was prepared (during the two hour waiting period of forskolin). The lumicycle recording media contained 30ml of F12 10%FBS, 1% PS and 30ul of luciferin. The vitamin D lumicycle recording media consisted of 30 ml F12 10% FBS, 1% PS, 30µl of 1nM vitamin D and 30µl of luciferin. The sixteen dishes were washed with 2ml of PBS. Eight of the dishes, four polished and four B + AE DCD titanium dishes had 1.5ml of the vitamin D recording media overlaid and grease sealed. The other eight dishes had 1.5ml of the lumicycle recording media overlaid without vitamin D and were grease sealed. The grease used to seal the dishes was Corning's high-pressure vacuum grease.

The sixteen dishes containing P3 BMSCs Per1::luc, were transported to the Lumicycle in aluminum foil, concealed from light until dishes were loaded in the lumicycle. The Lumicycle is a bioluminescence assay that measures the real time activation of luciferase. The Lumicycle is equipped with 4 photon counting photomultiplier tubes, each selected for low dark counts and

high sensitivity in the green portion of the spectrum at which luciferase emits light. Readings were taken every 10 minutes, as photon counts per second. All data is recorded on an attached computer for data processing and analysis. The Lumicycle is located in a dark room as the photo sensors are very sensitive to light. Each Lumicycle loading requires the dishes to be placed in the Lumicycle for 7 days with no media change.

Lumicycle Data Acquisition and Processing

All raw data was analyzed by comparing the average baseline photo count from each day between days one through four. Period was measured by the peak-to-peak, x-axis, distance in days while amplitude was taken as the peak to trough, y-axis. The period and amplitude measures were compared after performing a baseline subtraction and applying a polynomial fit line of sixteen with a smoothing of eighteen hours. Period and amplitude were compared across the different days and conditions.

Lumicycle Actimetrics a software program was used to perform the baseline subtraction (17) applied under a polynomial filter of 16 and a smoothing of 18 to produce well-defined peaks and amplitudes from the raw data. The process of baseline subtraction involves the use of a midline drawn between all peaks and troughs so as to normalize the circadian rhythm. The use of this technique allows for the visualization of well-defined peaks and troughs for definition of a rhythm. The polynomial number allowed for the midline to fit a more sensitively to a sinusoid curves that were circadian in nature. The smoothing allowed for the removal of noise.

Results

Two Lumicycle loadings are discussed in great detail in this paper. There were a total of three other Lumicycle loadings that were completed over the course of this experiment. All loadings used the three surfaces discussed (plastic, polished titanium, rough titanium) with and

without vitamin D. A smooth and rough titanium 32mm disks were placed in the Lumicycle as a control with no cells attached, to have a control for surface reaction to the Lumicycle photons. Results obtained from the three non-published loadings were very similar to the findings that are being analyzed and published in this paper.

Raw Per1 expression measures the amount of gene expression through photons per second, which were measured every ten minutes over the course of 5 days in the Lumicycle. The Raw Per1 expression (Figure 14) of polished titanium versus polished titanium with vitamin D BMSCs showed vitamin D slightly lowered the Per1 expression over all four days. This same trend was seen when comparing the rough titanium and the rough titanium with vitamin D, vitamin D (Figure 15), decreased the Per1 expression. What is very interesting is the photons per second measurement between the polished and rough titanium surfaces. The rough titanium surface had more than 50% reduction in photons per second each of the four days in comparison to the polished surface. Using the vitamin D condition all three surfaces are compared in Figure 16. Vitamin D condition was chosen to compare across all three surfaces, as this is most like healthy patients. Comparing the raw data from the polished and rough titanium groups, the polished vitamin D group had more Per1 expression than the rough vitamin D titanium group. Looking at the bar graph, it appears the rough surface expression is only one third of the expression on the plastic vitamin D group.

Baseline subtracted data normalizes the raw data by fitting a zero line midway between the peaks and troughs. The baseline subtraction data describes the peripheral rhythm of the BMSCs through peaks and troughs. Typically the parameters measured are amplitude and period. Amplitude is the measurement from peak to trough distance over days (horizontal axis) and photons per second for the vertical axis. Period is the measurement from peak to peak,

horizontal axis in days and vertical axis in photons per second. The baseline subtracted data (Figure 17) shows both the amplitude and period for the polished titanium and the polished titanium with vitamin D peripheral circadian rhythm. The polished vitamin D group suppresses the amplitude when compared to the polished titanium group. However, the period is maintained between both the polished titanium and polished titanium with vitamin D. The rough baseline subtracted data is drastically different than either the plastic or polished titanium groups (Figure 18). The rough baseline subtracted data appears significantly decreased in both the vitamin D group and rough titanium without vitamin D. The period is maintained but amplitude is just barely above the zero line.

Evaluating the average amplitude of polished with vitamin D and rough vitamin D surfaces(Figure 19) over the first three amplitudes, a 3x3 ANOVA found a significant surface effect F value 30.27 and P value 0.0001. There was also a significant difference between amplitudes 1, 2 and 3 F value 89.66 and P value 0.0001.

The average period of the baseline subtracted data (Figure 20) between polished with vitamin D and rough with vitamin D using a 3x3 ANOVA, shows a main effect between surfaces F value 15.09 and P value 0.0013.

Figure 21 nicely illustrates the peripheral circadian rhythms of the vitamin D groups examined. Period is maintained with in and in between the plastic and smooth surfaces examined with and without vitamin D. There is a distinct difference in amplitude between the three groups, the most dramatic difference being on the rough titanium surface. The rough titanium has also altered the period, there are no longer distinct peaks and troughs. Figure 22 shows all the peripheral circadian rhythms for all surfaces tested with and without vitamin D.

Figure 23 and 24 demonstrate the rough and smooth titanium surface reaction to photon expression with no cells attached.

Conclusion

Both titanium surfaces suppressed the expression of Per1 when compared to the raw Per1 expression on the plastic surface. The rough titanium surface significantly decreases raw Per1 expression, almost eliminating the gene expression. All surfaces retained a similar period regardless of vitamin D condition. Amplitude was decreased in both titanium surfaces compared to the BMSC amplitude on the plastic surface. The rough surface amplitude and period were most significantly decreased, almost negated. Titanium surfaces have a negative effect on Per1 expression and amplitude.

PART IV: Expression of circadian rhythm genes: an RT-PCR study

Specific Aim

1. Verify gene expression on CellTreat® and B+AE DCD surfaces using real time polymerase chain reaction (RT-PCR).

RT-PCR will be used to quantitate differences in mRNA expression between CellTreat® and B+AE DCD surfaces using seven Taqman probes: Id2, NPas2, Gapdh, Clock, BMal1, Per1 and Per2.

Methods and Materials

BMSCs were harvested, seeded, washed, passaged and recording media was used as if plates were being loaded in the Lumicycle, as previously described in Part I and III Methods and Materials. Passage 4 cells were used for the seeding on plastic and rough titanium surfaces. Cells were plated at 20,000cm^2 on three plastic 35mm dishes and three rough 32mm disks. Plates were placed in the 5% CO_2 and 37°C incubator. Cells were allowed to attached for four

days, on day two the media was changed. Day four the vitamin D condition was added and the cells were placed into an incubator with the same conditions as the Lumicycle. Forty-eight hours later the RNA was extracted from the BMSCs on the plastic and rough titanium surfaces (Figure 25). Protocol: Purification of Total RNA from Animal Cells Using Spin Technology and the RNeasy Mini Kit were used for RNA extraction from the six samples (15). The six RNA samples (3 plastic) and (3 rough titanium) were place in the -20° freezer. One week later the RNA samples were thawed on ice and were taken to the UCLA Geno Sequence Lab (36-125) to test the RNA purity. RNA purity was acceptable for two of the samples. Plastic sample concentration was 19.9ng/μl, 260/280 2.083 and 260/230 0.893. Rough sample concentration was 6.375ng/μl, 260/280 1.33 and 260/230 0.071. RNA samples were kept on ice while the master mix was fabricated using protocol of Clonetech cDNA Advantage RT-PCR kit (31). Thermocycler was used to fabricate cDNA. cDNA was frozen in -20° freezer. Appointment was schedule to complete RT-PCR one week later. cDNA was thawed on ice and necessary steps per Clonetech cDNA Advantage rt PCR kit were used to prepare the 96-well plate for RT-PCR. There were two samples and 7 gene probes and each sample was done in triplicate for each probe. The seven Taqman probes were: Id2, NPas2, BMal1, GAPDH, Clock, Per1 and Per2. The PCR conditions were Singleplex (Taqman Gene Expression Assay), Dye: FAM, and Quencher MGB. The 96-well plate was brought on ice to the UCLA Geno Sequence Lab Rm 36-125 and the standard cycle was ran on the ABI 7900 Taqman for 40 cycles. Results were downloaded from the Geno Sequence website (9).

Results

Per1, Per2, Clock, BMal1 and Id2 were all downregulated on the rough titanium surface. NPas2 was significantly upregulated by cells on the rough titanium surface (Figure 26). A T test

completed between plastic and rough samples for each probe and a p value of less than 0.05 was found in each surface comparison except in the Clock comparison.

Conclusion

The RT-PCR results validate the results of the raw and baseline subtracted data. Rough titanium surface downregulates circadian genes, specifically Per1, Per2, Clock, BMal1 and Id2. NPas2 was the only gene to be upregulated on the rough titanium surface. The gene expression on the plastic surface was not remarkable for an increase or decrease in gene expression. Peripheral circadian rhythm was in fact suppressed by the rough titanium surface.

Discussion

With each experimental result more questions appeared. What exactly is NPAS2 role in bone peripheral circadian rhythm? What does the increased gene expression of NPAS2 on the rough titanium mean? Is there a significance to osseointegration because the all five out of the six clock genes are downregulated? Are Clock genes except, NPAS2, downregulated when an implant is successfully integrating? Clinically, how does this information translate to implant patients? What role or differences are seen in peripheral circadian genes versus SCN circadian genes and their functions in bone and wound healing? These are just a few of the questions that came to mind after examining the data from my experiments.

In the Mengatto study, NPAS2 and cartilage ECM genes were upregulated in the successful implant model, with vitamin D (4). NPAS2 stands for neuronal PAS domain protein 2, which is a transcription factor expressed primarily in the mammalian forebrain (19). It is highly related in primary amino acid sequence to CLOCK, which has been discussed as a transcription factor expressed in the SCN that heterodimerizes with BMAL1 and regulates circadian rhythm (19). NPAS2 is a member of the basic helix-loop-helix PAS family of

transcription factors, involved in the regulation of circadian rhythm (21). The primary molecular target of NPAS2 is Per2, which was also significantly modulated (upregulated) by vitamin D deficiency (4).

It has been suggested NPAS2 is a paralog of CLOCK. Paralogs are genes that related by duplication within a genome but evolve new functions (23). CLOCK and NPAS2 can independently heterodimerize with BMAL1 in SCN to maintain molecular and behavorial rhythmicity (22). Studies are unable to distinguish whether NPAS2 normally functions to regulate circadian gene expression in the SCN of wild type mice or whether NPAS2 only have functionally relevant effects on gene expression in the absence of CLOCK (22). Studies also have shown that CLOCK deficient mice continue to exhibit a robust behavorial and molecular rhythm (22). In this particular study NPAS2 could be functionally substituted for CLOCK in the master brain clock in mice to regulate circadian rhythmicity (22). The molecular defects in $NPas2^{-/-}$ mice are more subtle than those observed in CLOCK deficient mice, suggesting CLOCK normally has a more prominent role than NPAS2 in controlling central circadian gene expression (22). $NPas2^{-/-}$ knockout mice display a slightly shorter circadian period, altered response to perturbations in the light-dark cycle, a dampened mPer2 rhythm and BMal1 levels, although rhythmic, were increased throughout the circadian day (22). These circadian phenotypes have been proposed to be a result of disrupted crosstalk between the forebrain and SCN clocks, not a result of NPAS2 deficiency in the SCN (22). NPAS2 and CLOCK acted independently when evaluating the rough titanium RT-PCR results in peripheral circadian rhythm.

Recall the molecular pathway of Per1 and Per2, which is best characterized as a negative feedback loop. The common mammalian circadian molecular mechanism begins with the formation of the circadian rhythm initiating Clock/Bmal1 complex (17). This heterodimer binds

to the E-box in the nucleus and promotes the transcription of genes period homolog (Per) 1, 2, 3 and cryptochrome (Cry) 1, 2 as well as Rev-Erb nuclear orphan receptors and retinoic acid related orphan receptors (10). Per and Cry translated proteins then dimerize in the cytoplasm and are phosphorylated by casein kinase, which allows for Per/Cry dimmer to trans-locate back into the nucleus and inhibit the BMAL/CLOCK heterodimer over a 24 hour period (10). The specific phosphorylation of Per allows for its subsequent degradation after it has completed it nuclear inhibition (18). Peripheral circulating Per1 would be higher during the morning and levels would be decreased at night due to the negative feedback loop. Therefore, the RT PCR results of PER1, PER2, BMAL1 and CLOCK on rough titanium are logical. If there is less CLOCK/BMAL1 to bind in the nucleus for transcriptions, there will be less circulating PER1, PER2, CRY1 and CRY2 available in tissues. Deficiencies seen in clock genes can cause these mutant mice to have abnormal bone formation, tumor surveillance, and metabolic pathways may have no causal relationship with the circadian clock. The rigorous discrimination between clock function and clock gene function is not a trivial matter (24). A considerable body of evidence has accumulated for relationships to numerous diseases derived from polymorphisms and deviations in gene expression in humans and from animal models (25). The involvement of a specific gene variant in the etiology of a disease or disorder is not equally evident in each of these studies and controversies have arisen with specific details or claims, but the evidence for the profound (Table 10) importance of a well-functioning circadian oscillator system in the maintenance of health is already overwhelming (25). Disruption in circadian genes leads to deregulation of pathways, cell cycle control, tumor growth and a variety of other problems but could this downregulation seen in BMSCs clock genes on titanium indicated osseointegration?

In literature there are both in vitro and animal in vivo studies to evaluate circadian genes in the SCN neurons (master clock in the brain) and circadian genes in peripheral cells. In mammals, the circadian timing system is composed of virtually as many clocks as there are cells, as most cells harbor self-sustained and cell-autonomous circadian oscillators (24). Both in the SCN and peripheral cells, the rhythm-generating molecular circuitry is based on a delayed transcriptional/translational feedback loop involving essentially the same core clock components (24). In spite of the resemblances between central and peripheral clocks, the term master and slave oscillators are still justified (24). Phases of peripheral oscillators exhibit large differences in SCN-lesioned animals. Organs such as a liver, need a functional SCN to maintain phase coherence between hepatocytes of the liver as peripheral oscillators do not appear to be coupled via paracrine communication signals (24). The loss of BMSCs amplitude between the three different surfaces could be due to the loss of cell-to-cell rhythmicity due to the lack of a master clock. It has been reported that transplantation of an SCN into and SCN lesioned animal can restore phase coherence of circadian gene expression in the liver, kidney, and skeletal muscle but not in the heart, spleen, or adrenal medulla (24). Synchronization of the heart, spleen and adrenal medulla perhaps requires inputs from the peripheral nervous system, which cannot be restored by an implanted SCN (24). Resilience of cellular clocks to changes in temperature and gene expression may be even more important in peripheral cell types than in the SCN. SCN oscillators are more resilient to perturbances. Peripheral clocks are rather autistic and must relay on cell-autonomous robustness (24). Synchronization of peripheral clock genes by the SCN remain largely unknown and many signaling pathways are expected to be involved in the phase entrainment of peripheral clocks (24). Hence, the elimination of a single pathway is unlikely to significantly affect the steady-state phase of circadian clocks (24). A more sensitive approach

would be the recording of phase-shifting kinetics, recording living animals. Developing a noninvasive whole-body imaging technique to allow the recording of central and peripheral gene expression patterns in freely moving animals (24). This is a large limitation in my BMSC *Per1:luc* study where cells were explanted. To be able to measure *Per1* expression or to look for mRNA expression after a titanium implant is surgically placed into a mouse or rat femur would be a more realistic and accurate model to compare clinically.

One other interesting point of discussion is the connection between Per1 and melatonin. Melatonin is a principal tryptophan derived indolamine secreted by the pineal gland, which undergoes marked temporal variation in secretion and drives a wide range of rhythmic physiology (26,27). In mammals, the synthesis and secretion of pineal melatonin occurs at night, under the control of the SCN. The variation of this nocturnal signal varies in proportion to the length of the night, and hence secretion transduces both daily and seasonal time throughout the body (27). Melatonin has antioxidant properties, free radial scavenging abilities and also can inhibit bone resorption by suppression of osteoclast activity (26). Melatonin has been shown to increase osteoblast proliferation and differentiation in vitro. A study was designed to stimulate peri-implant bone response with melatonin during implant placement (20 implants) in rabbit tibae (26). It was found direct melatonin (3mg) locally administered to the implant osteoctomy site significantly increased the trabecular BIC and trabecular density compared to the control group. Cortical BIC and cortical bone density was decreased in the melatonin groups. There conclusion within the limitation of the study was local melatonin application at the time of implant placement may induce more trabecular bone density and trabecular bone contact with the titanium implant (26).

Johnston et al. using a sheep model evaluated the effect of melatonin and circadian rhythm genes. It was found that melatonin acutely inhibits the endogenous elevation and expression of multiple clock genes, specifically BMAL1 and Per1 (Figure) (27). It would have been very interesting to compare gene expression from the implant melatonin rabbit experiment to evaluate melatonin effect on Per1 in the presence of a rough titanium surface.

There is emerging data that has demonstrated NPAS2 has a substantial impact on tumor related biologic pathways, possibly through regulation of cancer-related genes, such as those involved in cell cycle checkpoint and DNA repair (28). The expression of NPAS2 may serve as a strong prognostic biomarker, and the genotype of NPAS2 may be marginal prognostic biomarker, in addition to its association with breast cancer risk (28). This article was one of the first reports relating expression levels of circadian gene and cancer survival. Further examination of NPAS2 and other circadian genes as prognostic biomarkers and cancer type is warranted (28). There is no published data evaluating circadian rhythm genes in mammals in regards to bone wound healing.

The overwhelming fact remains that hundreds of genes are expressed in a cyclic manner and most physiology follows a daily rhythm. This knowledge has been largely ignored in the clinic, and only a few pioneers are making efforts to explore this temporal information designing better therapies (24). There is much to be explored between health and circadian gene expression as well as disease and circadian gene expression. The gene suppression of ID2, BMAL1, PER1, PER2 and CLOCK by rough titanium; and significant upregulation of NPAS2 on rough titanium was unexpected. Followed by the finding that a rough titanium substrate has a negative effect on Per1 amplitude and period. Bone clock gene suppression may indicate

osseointegration. NPAS2 elevation or expression may be a novel way to determine implant osseointegration.

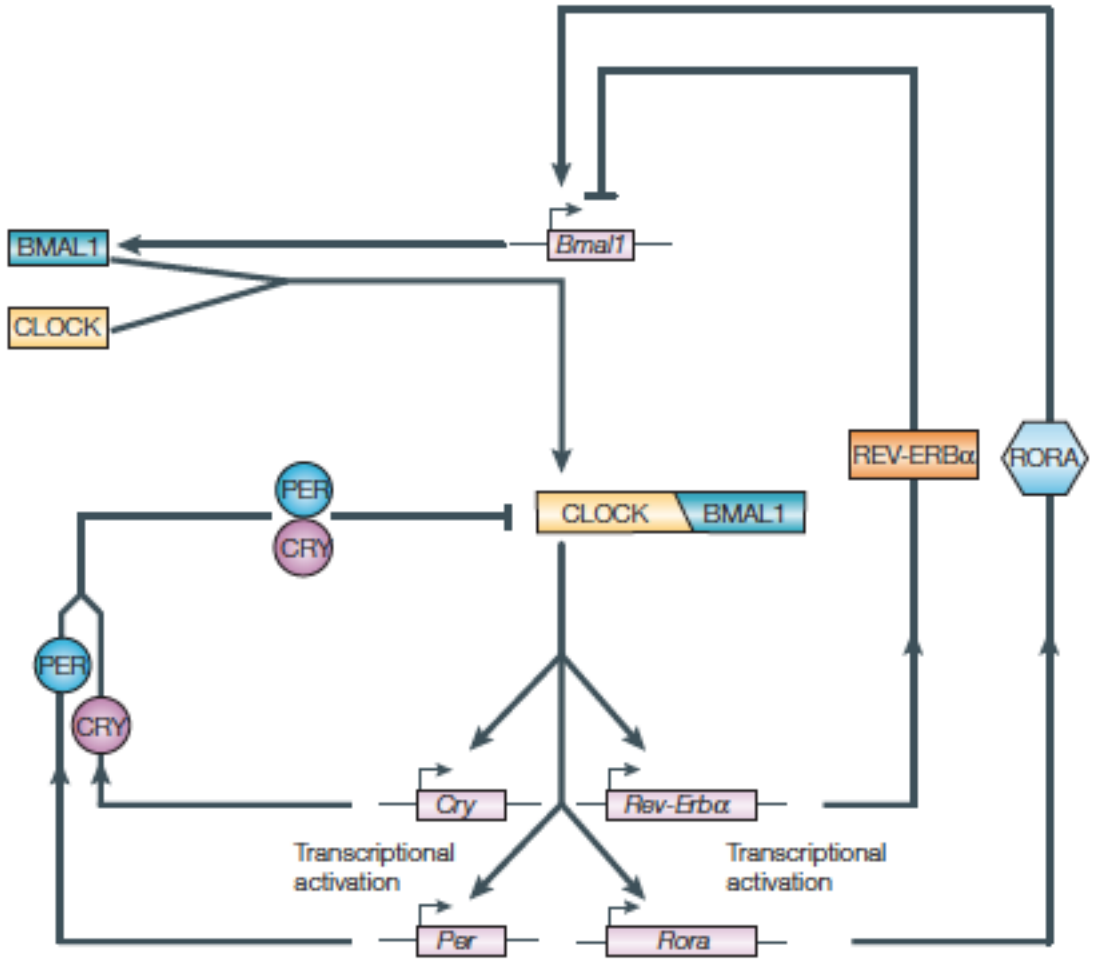

Figure 1. CLOCK/BMAL-1 Molecular Pathway (5)

Table 1. Processes Controlled by Pacemakers and Oscillators

Table 1 | **Examples of processes that are controlled by pacemakers and oscillators in model organisms**

Organism	Oscillator or tissue with pacemaker function	Processes regulated by pacemaker	Other oscillators present?	Processes regulated by other oscillators
Synechoccus elongatus	Kai periodosome	Cell division, photosynthesis, carbohydrate synthesis, gene expression, amino-acid upatake	Predicted, but not yet described	Gene expression?
Neurospora crassa	FRQ/WC oscillator	Conidiation, gene expression	FLO Other oscillators (not yet described)	Gene expression Gene expression, conidiation?
*Drosophila melanogaster**	Ventral lateral neurons Olfactory sensory neurons Autonomous oscillators in other tissues?	Locomotor activity Odour-dependent electrophysiological responses Gene expression, other rhythms?	N/A	N/A
Mammals	SCN	Locomotor activity, electrical firing, cytosolic calcium levels, 2-deoxyglucose uptake, neuropeptide secretion, gene expression	Heart Lung Liver Kidney Fibroblasts Pineal gland	Heart rate, systolic blood pressure, vasodilation, gene expression Gene expression Metabolism, vesicular trafficking, detoxification, gene expression Gene expression Gene expression Melatonin levels
Birds	Retina SCN Pineal gland	Melatonin levels Noradrenaline levels, electrical firing, sympathetic tone Melatonin levels	Predicted, but not yet described	Gene expression?

*Oscillators in flies do not meet the classic criteria of a pacemaker; however, they are not dependent on other oscillators for their entrainment or function, and autonomously control rhythmic outputs — therefore they have pacemaker properties. FLO, FRQ-less oscillator; FRQ/WC, *frequency/white-collar* oscillator; SCN, suprachiasmatic nucleus.

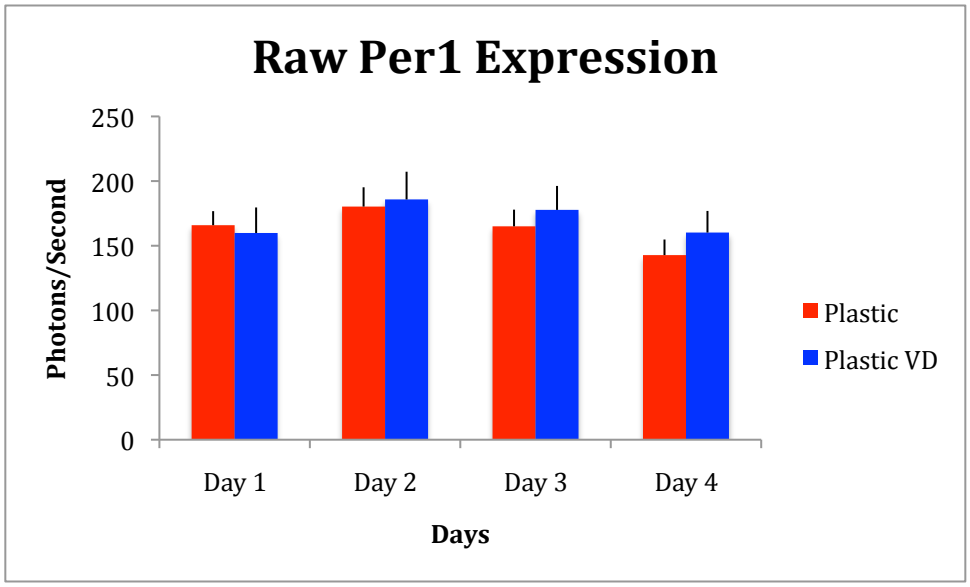
Raw Per1 Expression
250
200
150
100
50
0
Photons/Second
Day 1
Day 2
Day 3
Day 4
Days
Plastic
Plastic VD

Figure 2.

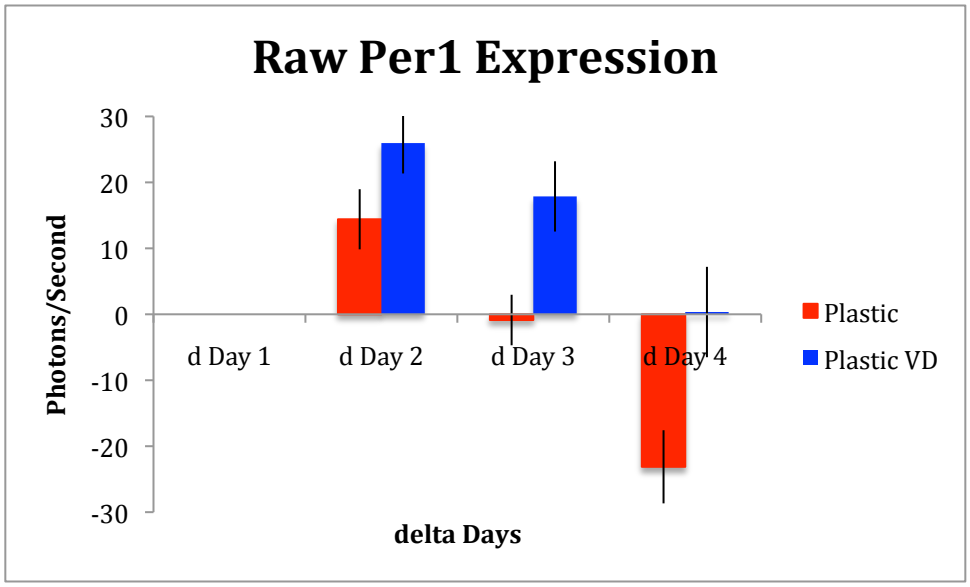
Raw Per1 Expression
30
20
10
0
-10
-20
-30
Photons/Second
d Day 1
d Day 2
d Day 3
d Day 4
delta Days
Plastic
Plastic VD

Figure 3.

Table 2. d Days Plastic/Plastic VD

	Plastic	Plastic VD	Plastic SD	Plastic VD SD
d Day 1	0	0	0	0
d Day 2	14.40466738	25.9590406	4.558123458	4.606369341
d Day 3	-0.869662486	17.87124373	3.829694051	5.324135957
d Day 4	-23.12324756	0.343344423	5.543829179	6.851054592

T Test d Day 2 Plastic vs Plastic VD	0.00592083
T Test d Day 3 Plastic vs Plastic VD	0.000621554
T Test d Day 4 Plastic vs Plastic VD	0.000892995

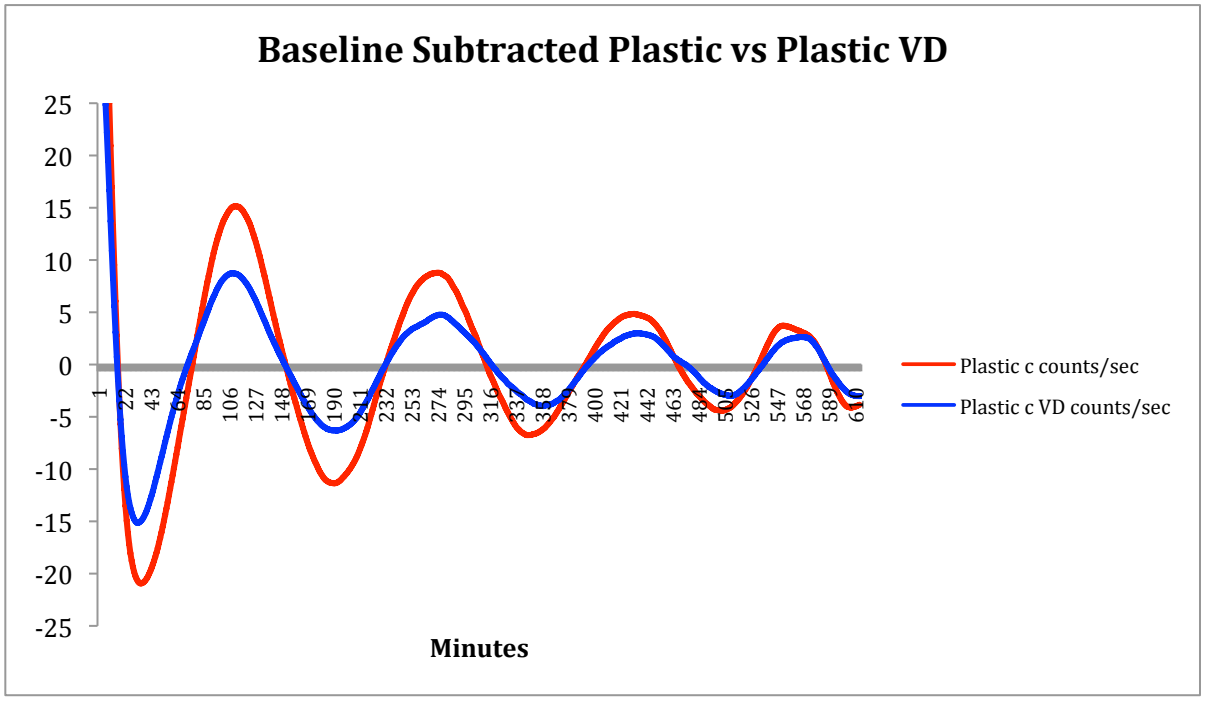

Figure 4. Circadian Rhythm of Plastic and Plastic with Vitamin D

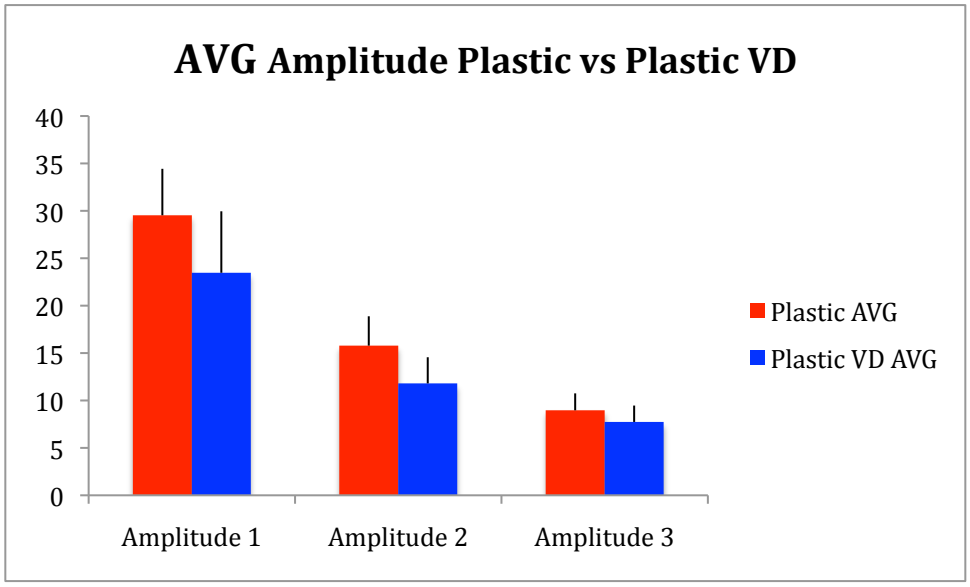
AVG Amplitude Plastic vs Plastic VD
40
35
30
25
20
15
10
5
0
Amplitude 1
Amplitude 2
Amplitude 3
Plastic AVG
Plastic VD AVG

Figure 5.

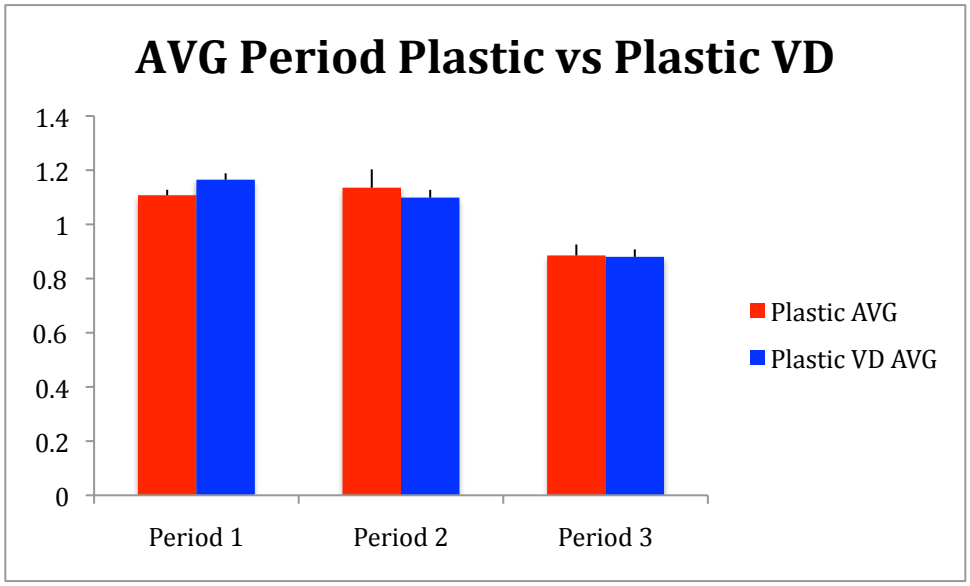
AVG Period Plastic vs Plastic VD
1.4
1.2
1
0.8
0.6
0.4
0.2
0
Period 1
Period 2
Period 3
Plastic AVG
Plastic VD AVG

Figure 6.

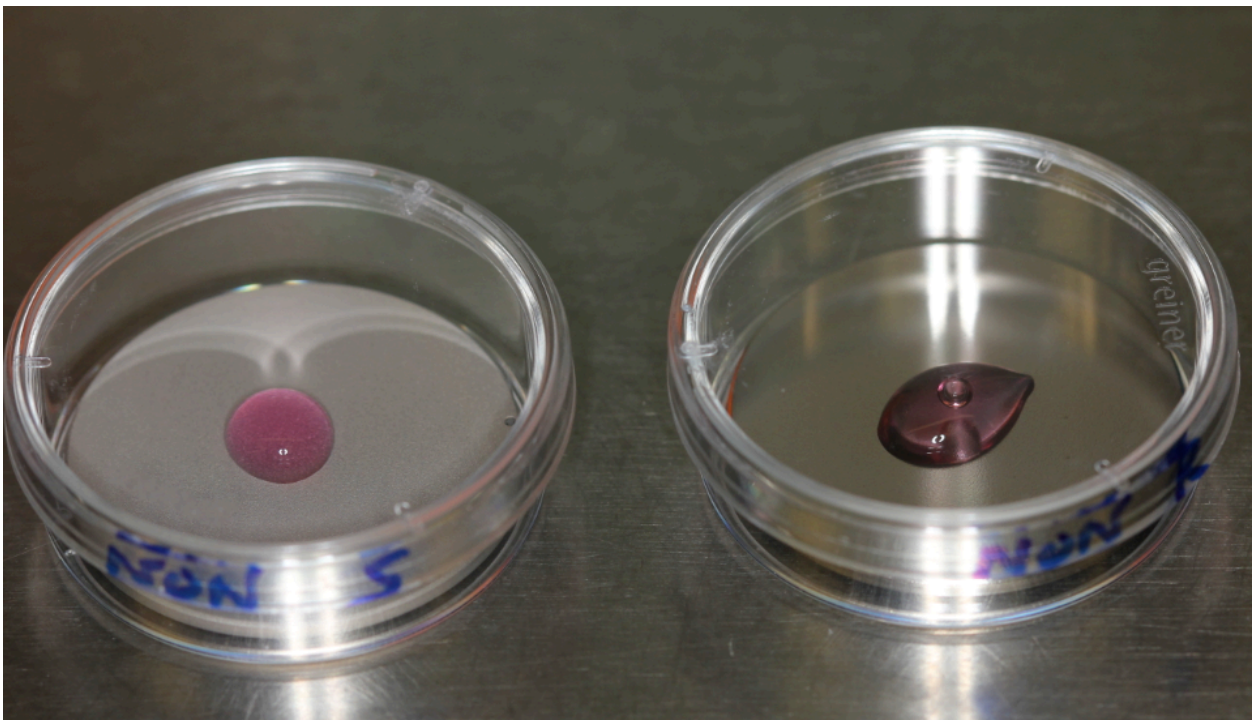

Figure 7. Photograph of Rough and Polished Titanium

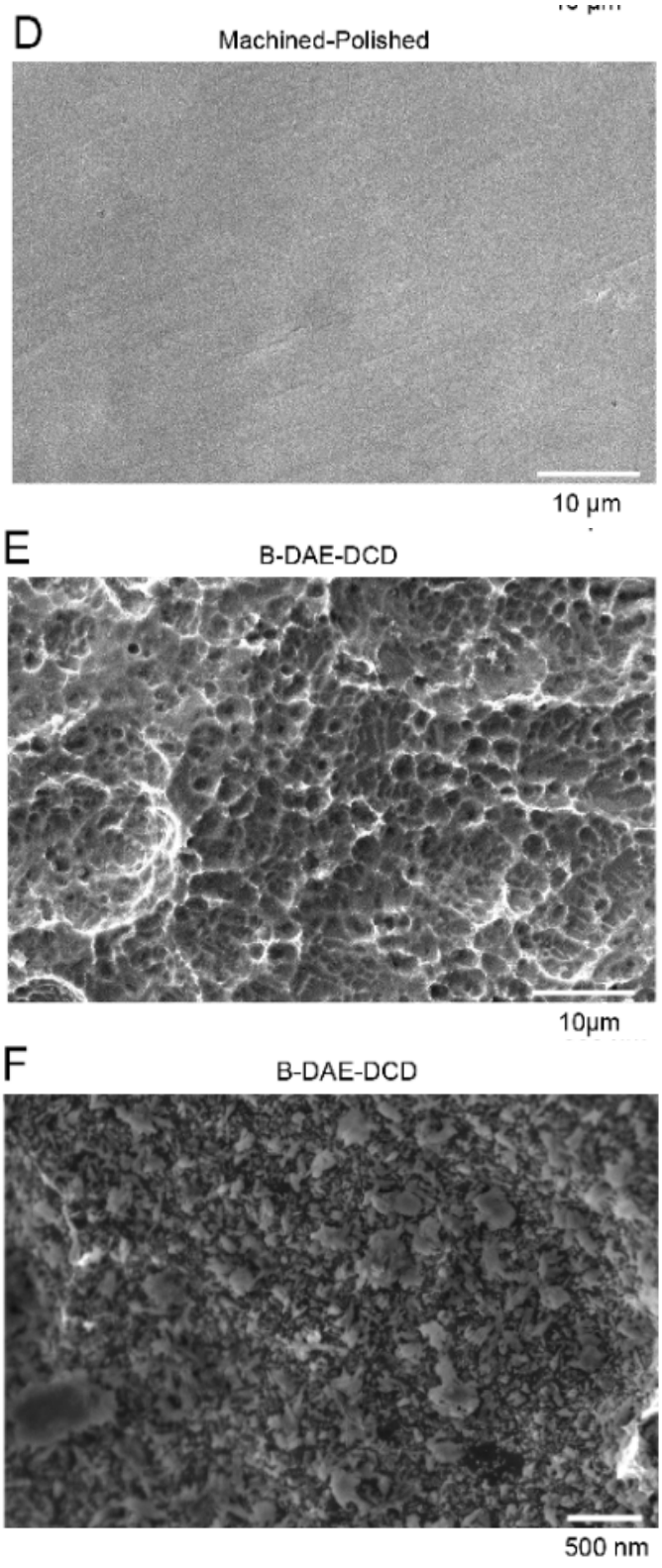

Figure 8. SCM

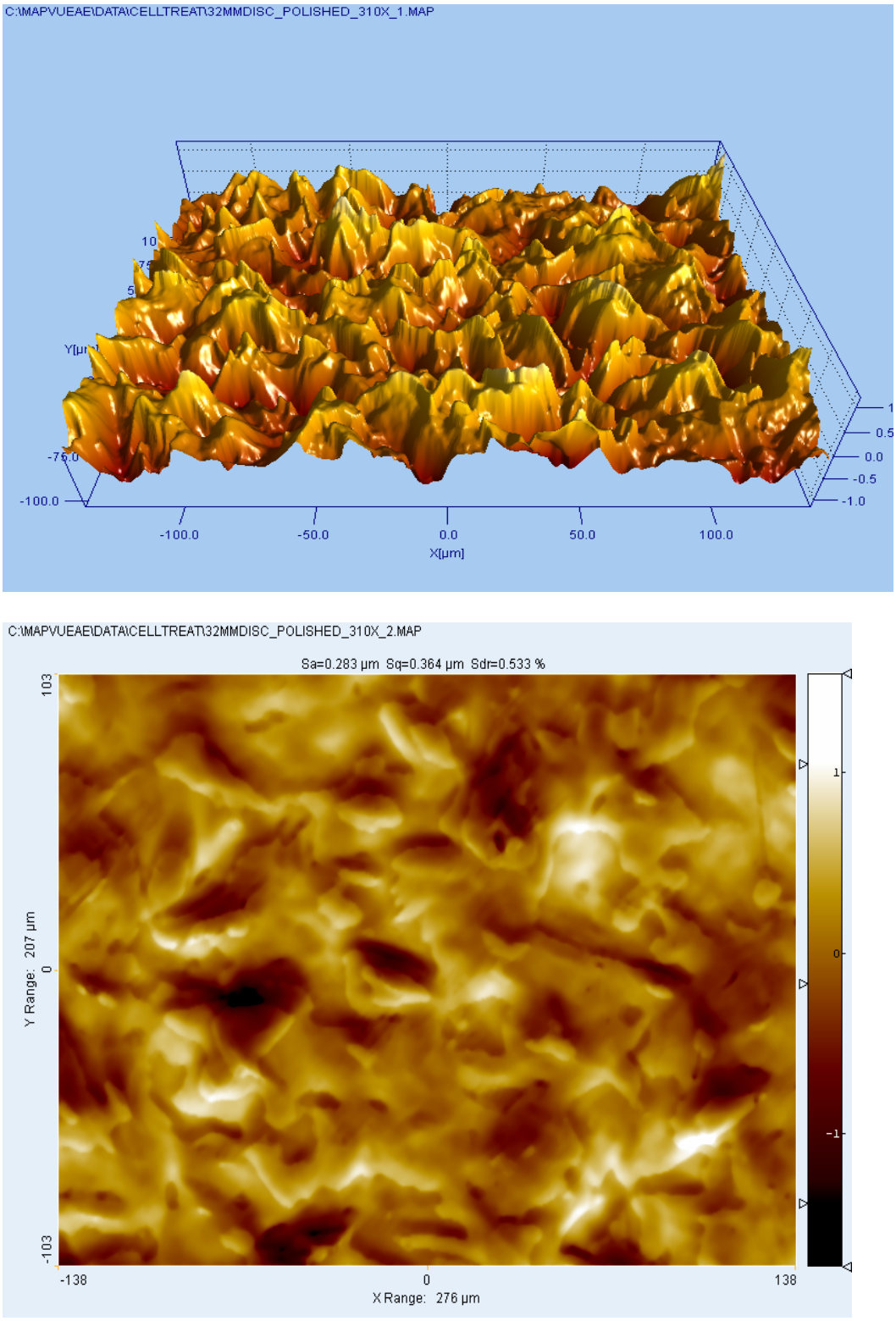

Figure 9. Profilometry Polished Titanium

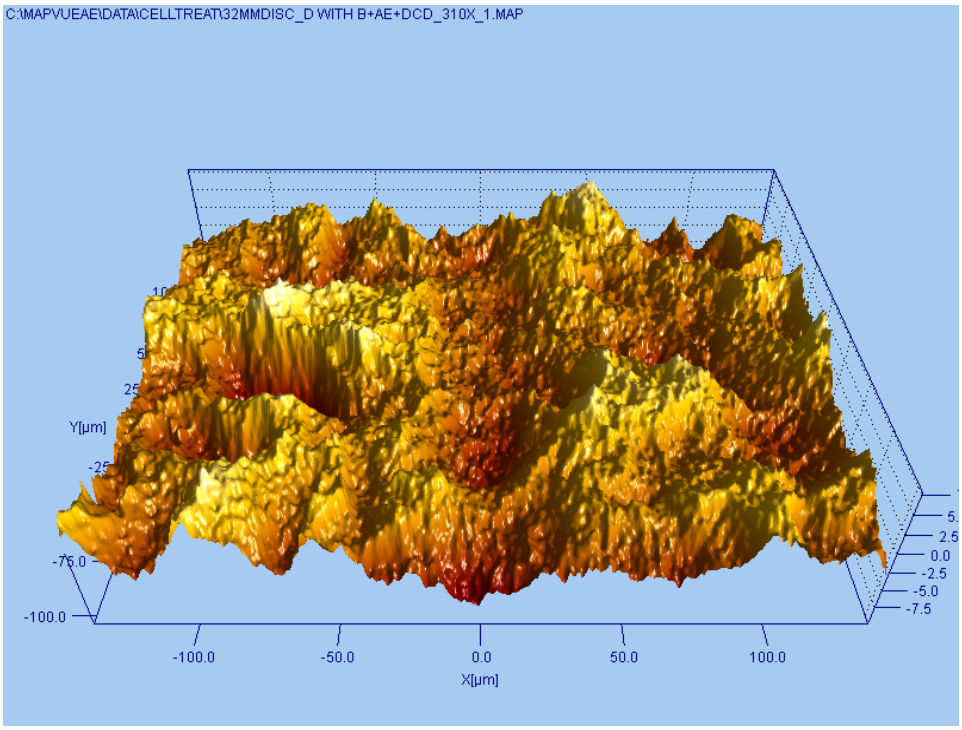

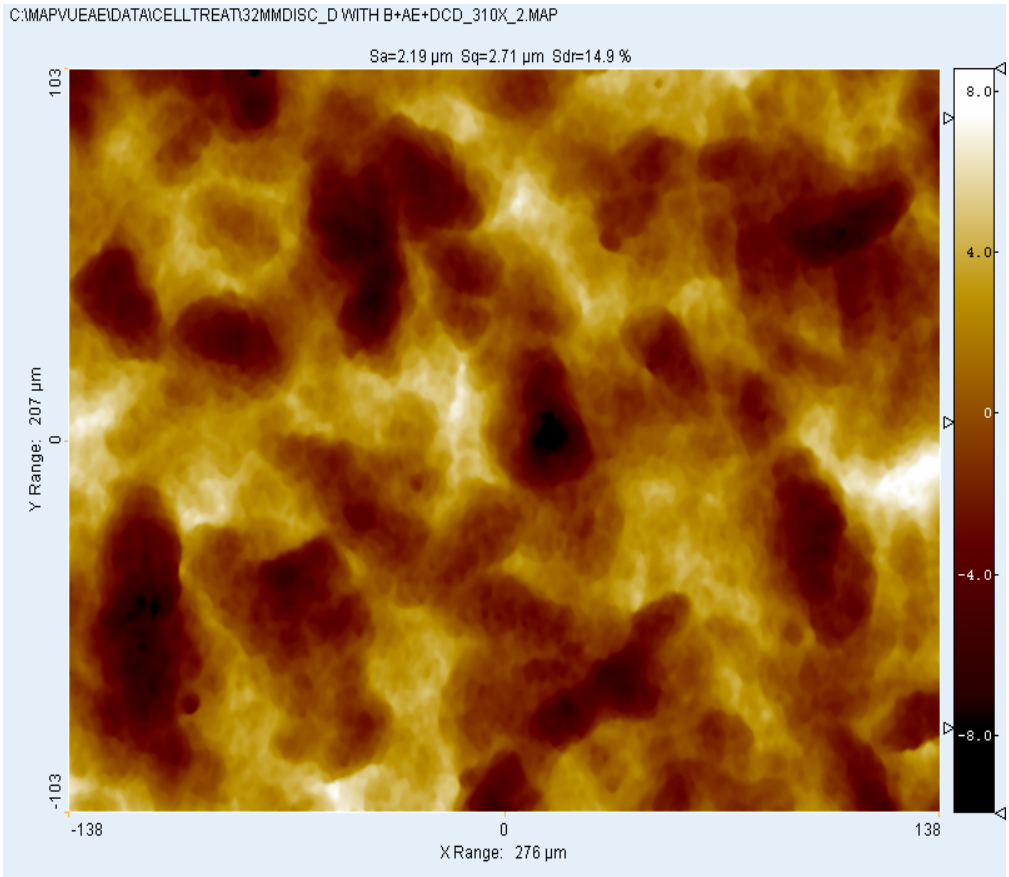

Figure 10. Profilometry Rough Titanium

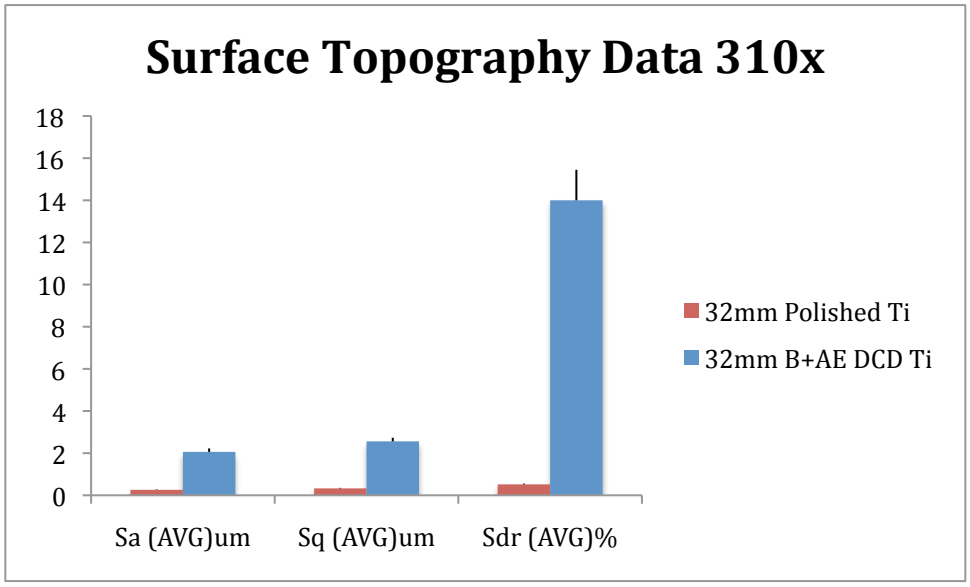
Surface Topography Data 310x
18
16
14
12
10
8
6
4
2
0
Sa (AVG)um
Sq (AVG)um
Sdr (AVG)%
32mm Polished Ti
32mm B+AE DCD Ti

Figure 11.

Table 3.

Surface Topography of Implants from Four Major Companies

Company	World Market Share	Implant	Sa (um)	Sdr (%)	Sq
3i	15-20%	Osseotite	0.68	27	
		Nanotite	0.5	40	
		Prevail (Ti-6AI-4V)	0.3	24	
Dentsply/Astra	12%	TiOblast	1.1	31	
		Osseospeed	1.4	37	
Nobel Biocare	30%	TiUnite	1.1	37	
Straumann	25%	SLA old batch	1.5	34	
		SLA new batch	1.78	97	
		SLActive	1.75	143	
		32mm Polished Ti	0.259	0.5186	0.3278
		32mm B+AE DCD Ti	2.06	14	2.56

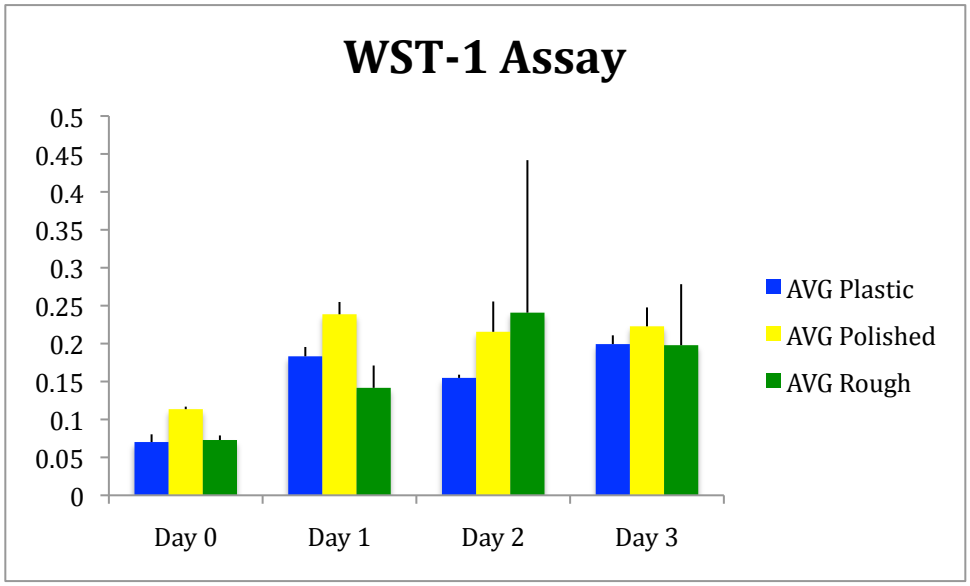
WST-1 Assay
0.5
0.45
0.4
0.35
0.3
0.25
0.2
0.15
0.1
0.05
0
Day 0
Day 1
Day 2
Day 3
AVG Plastic
AVG Polished
AVG Rough

Figure 12.

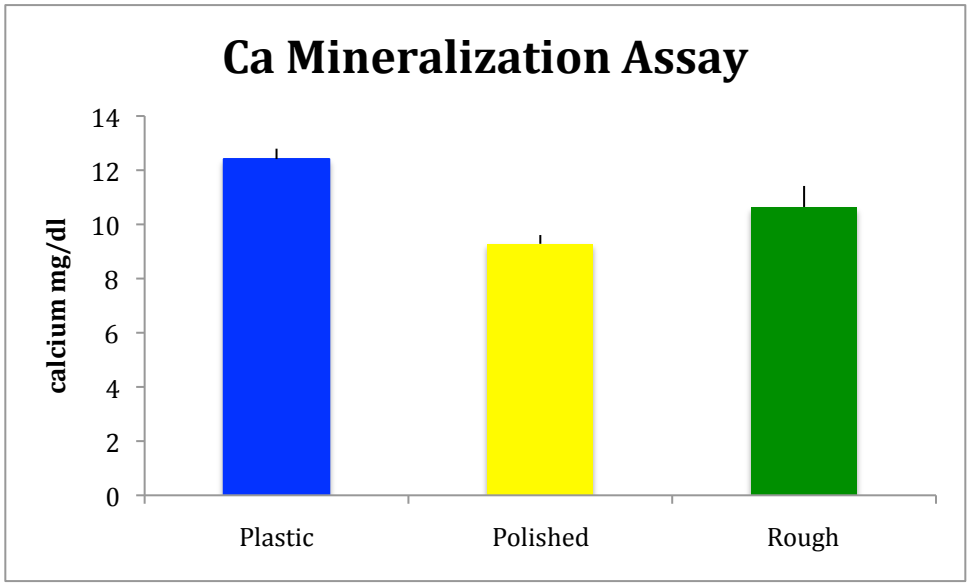
Ca Mineralization Assay
calcium mg/dl
14
12
10
8
6
4
2
0
Plastic
Polished
Rough

Figure 13.

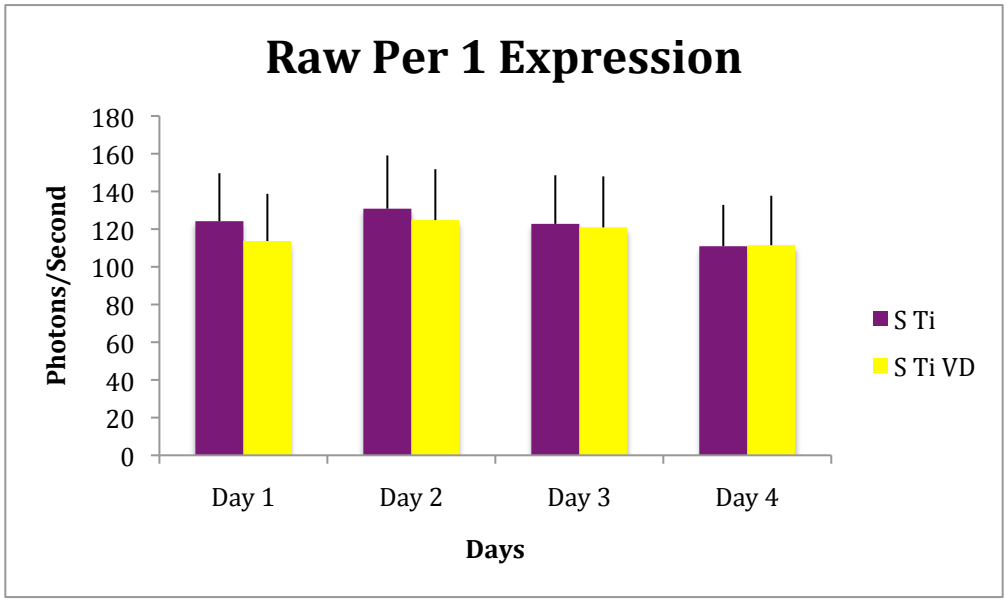
Raw Per 1 Expression
Photons/Second
180
160
140
120
100
80
60
40
20
0
Day 1
Day 2
Day 3
Day 4
Days
S Ti
S Ti VD

Figure 14.

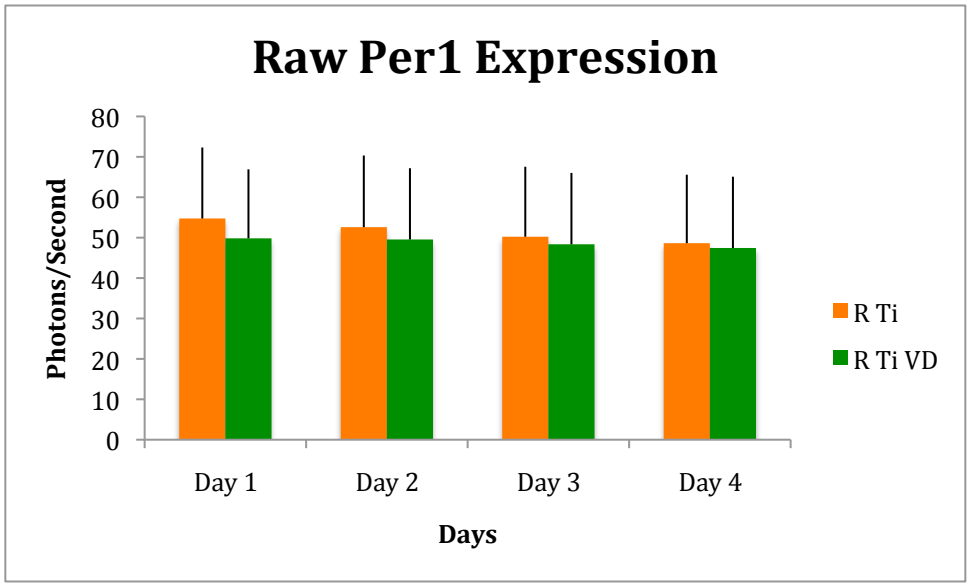
Raw Per1 Expression
Photons/Second
80
70
60
50
40
30
20
10
0
Day 1
Day 2
Day 3
Day 4
Days
R Ti
R Ti VD

Figure 15.

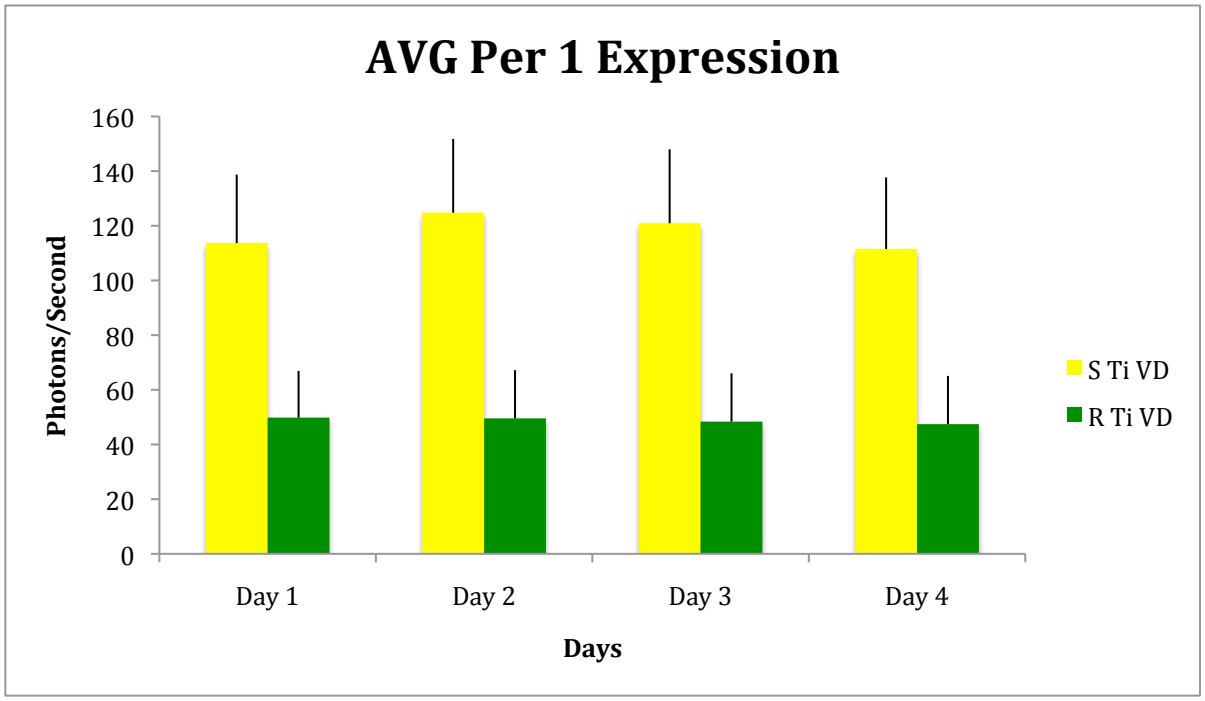

Figure 16. Average Per1 Expression Polished Vitamin D and Rough Vitamin D

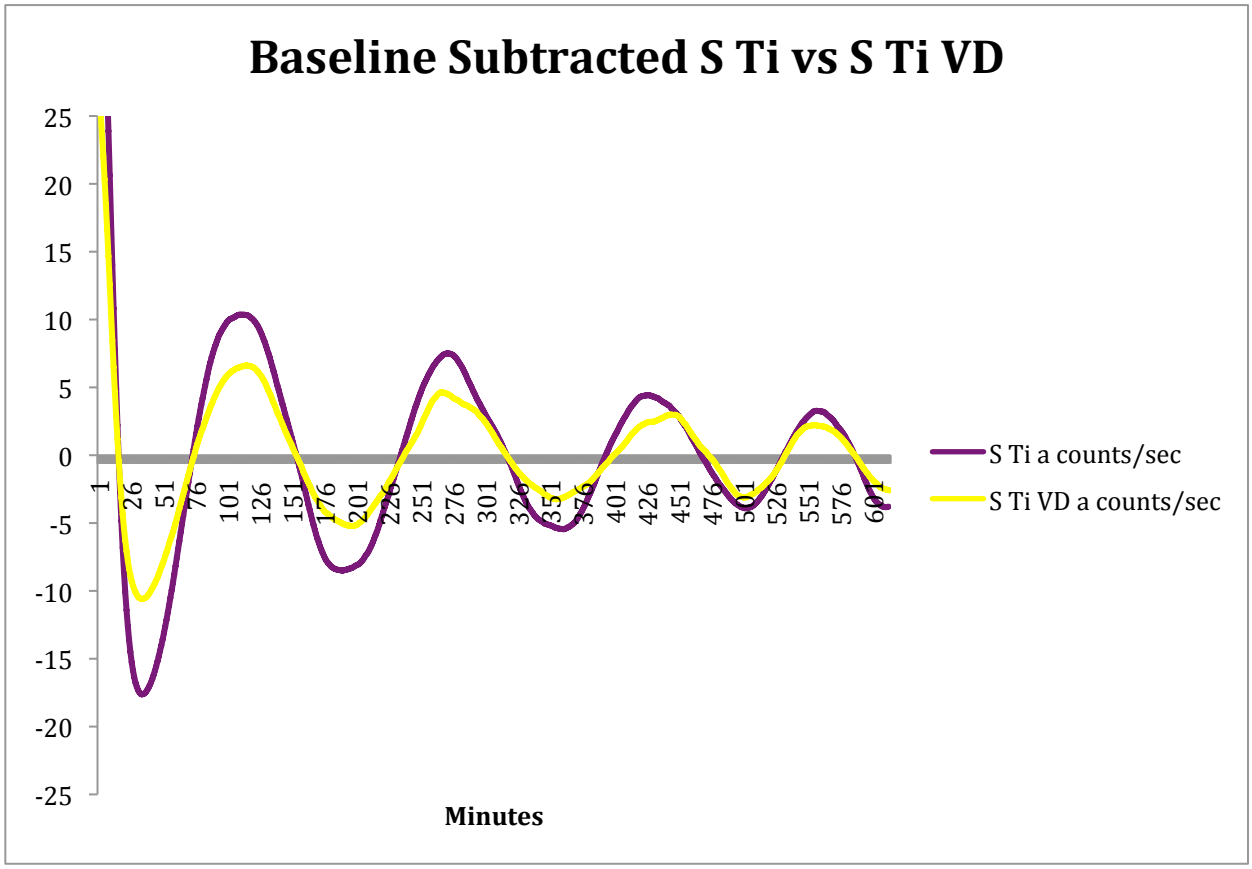

Figure 17. Circadian Rhythm of Polished and Polished with Vitamin D

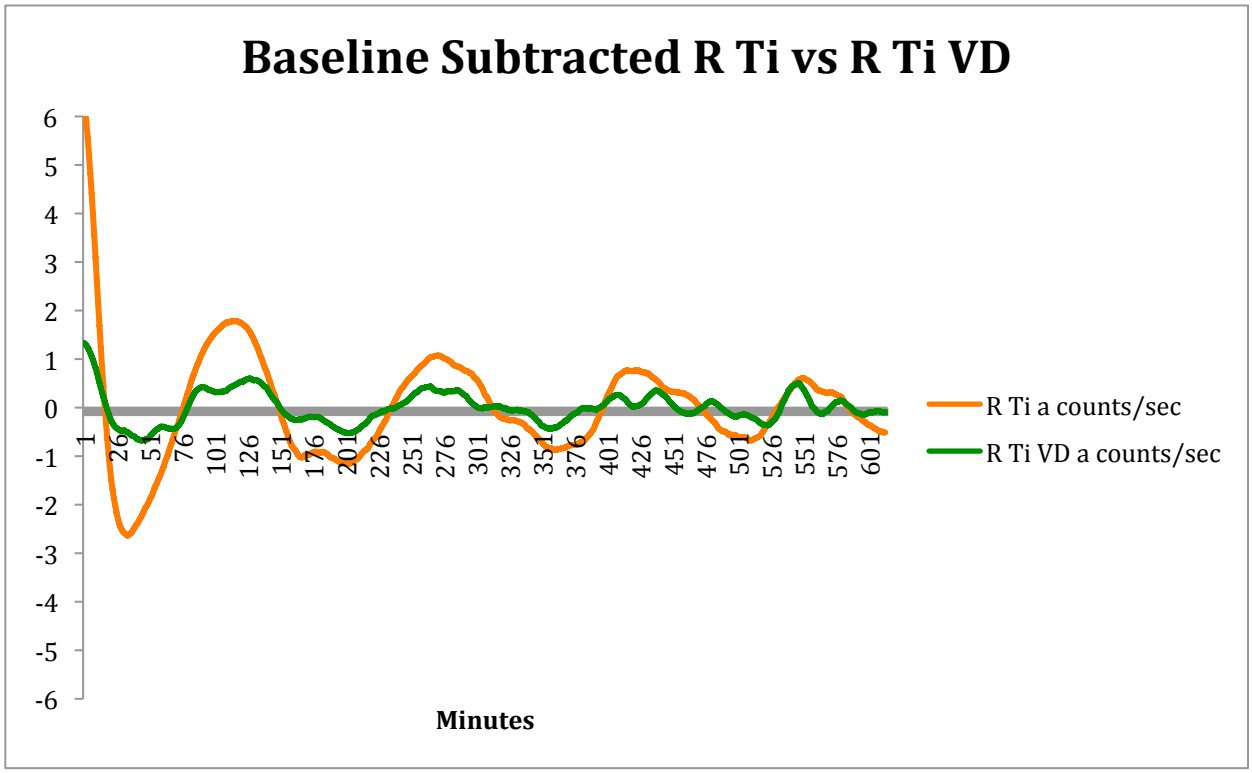

Figure 18. Circadian Rhythm of Rough and Rough Vitamin D

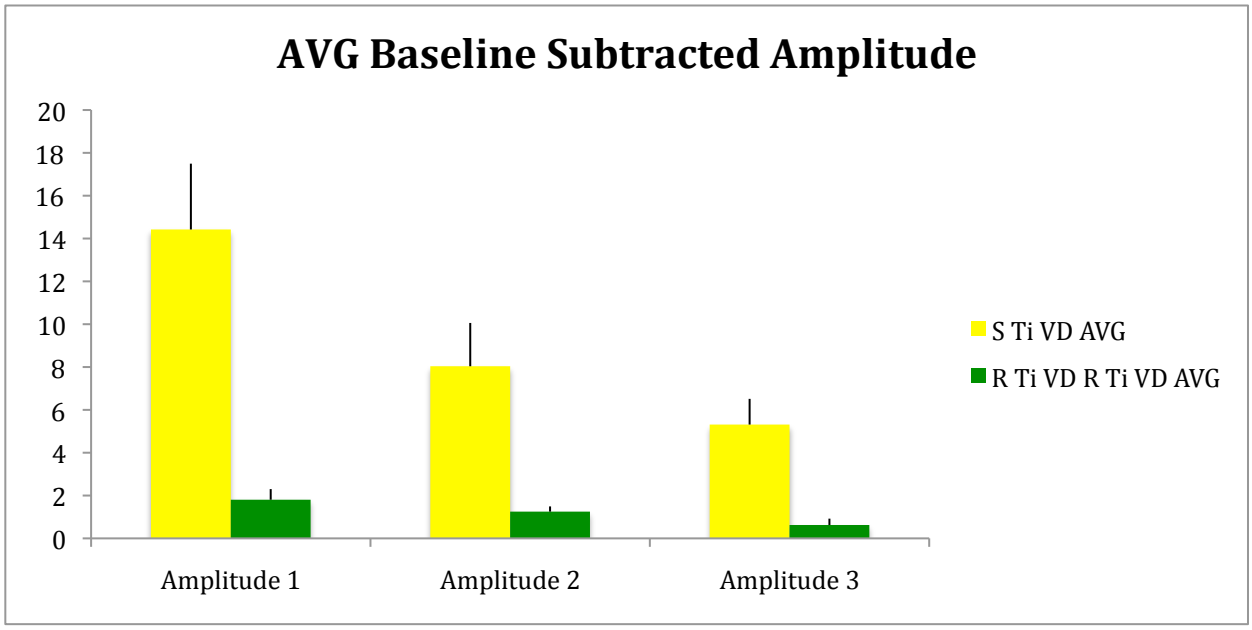
AVG Baseline Subtracted Amplitude
20
18
16
14
12
10
8
6
4
2
0
Amplitude 1
Amplitude 2
Amplitude 3
S Ti VD AVG
R Ti VD R Ti VD AVG

Figure 19.

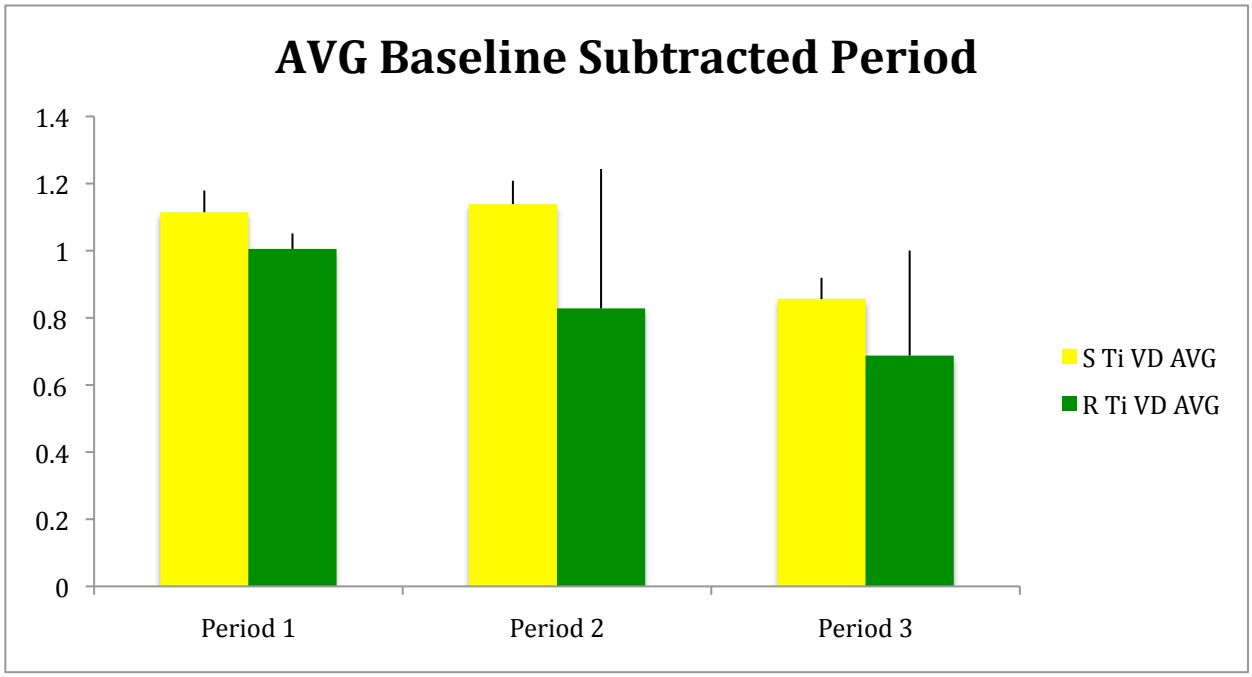
AVG Baseline Subtracted Period
1.4
1.2
1
0.8
0.6
0.4
0.2
0
Period 1
Period 2
Period 3
S Ti VD AVG
R Ti VD AVG

Figure 20.

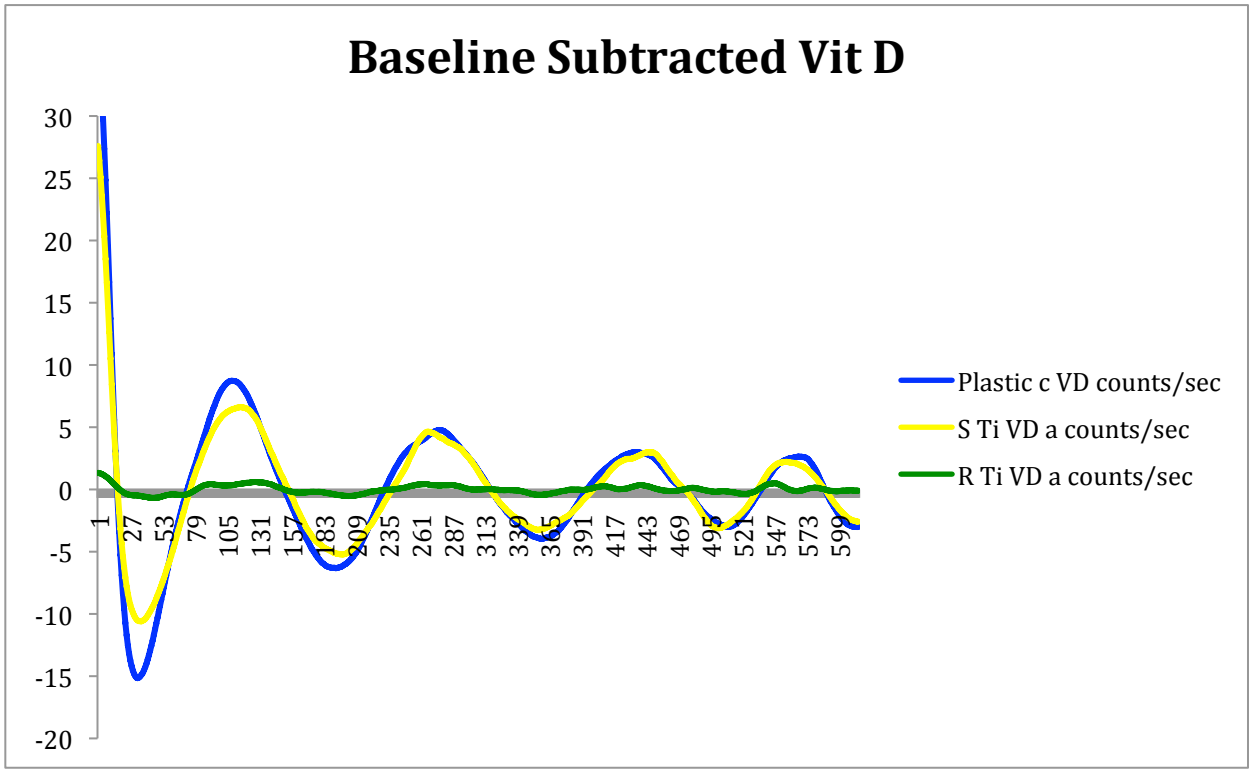

Figure 21. Circadian Rhythm of Surfaces with Vitamin D

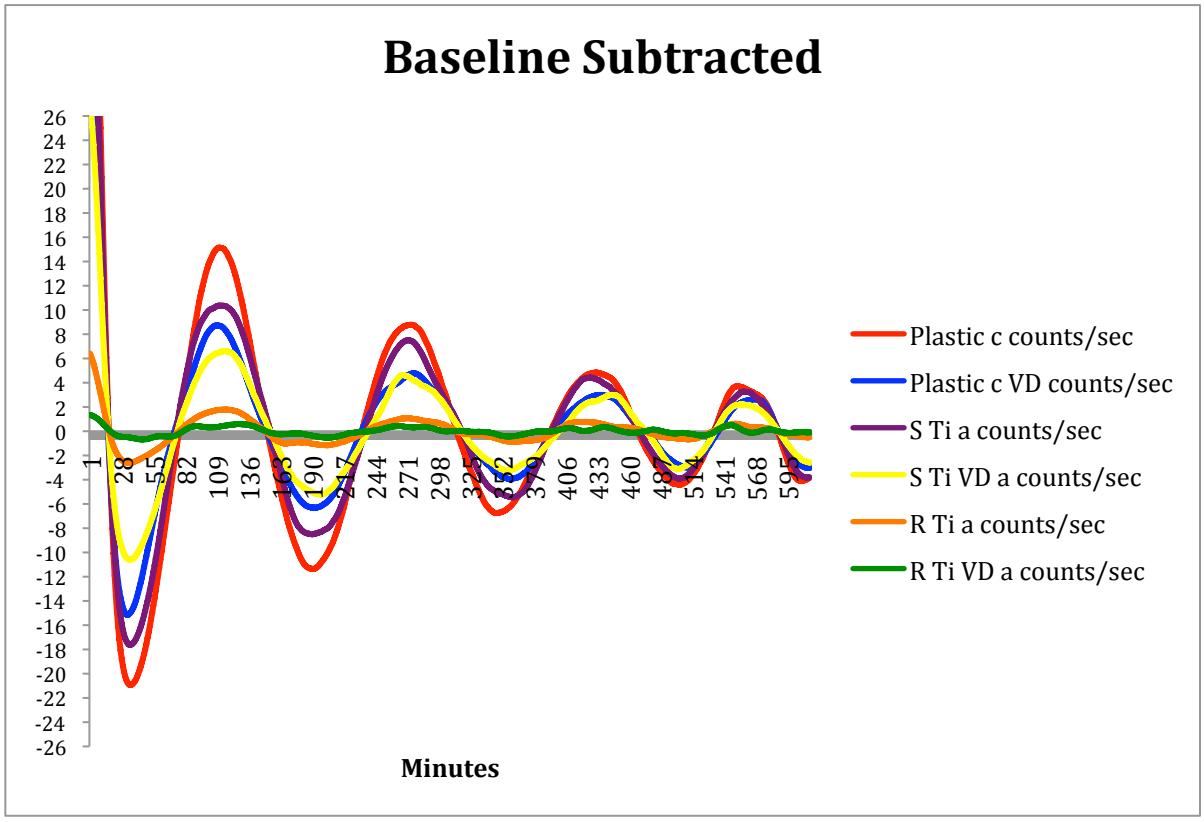

Figure 22. Circadian Rhythm of All Surfaces and Conditions

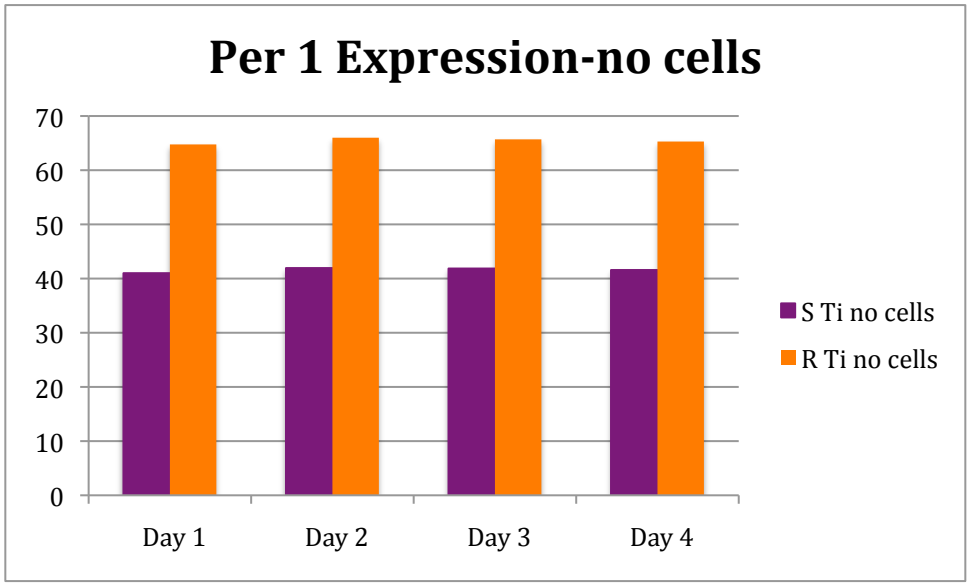

Figure 23. Per 1 Expression of Titanium with no cells

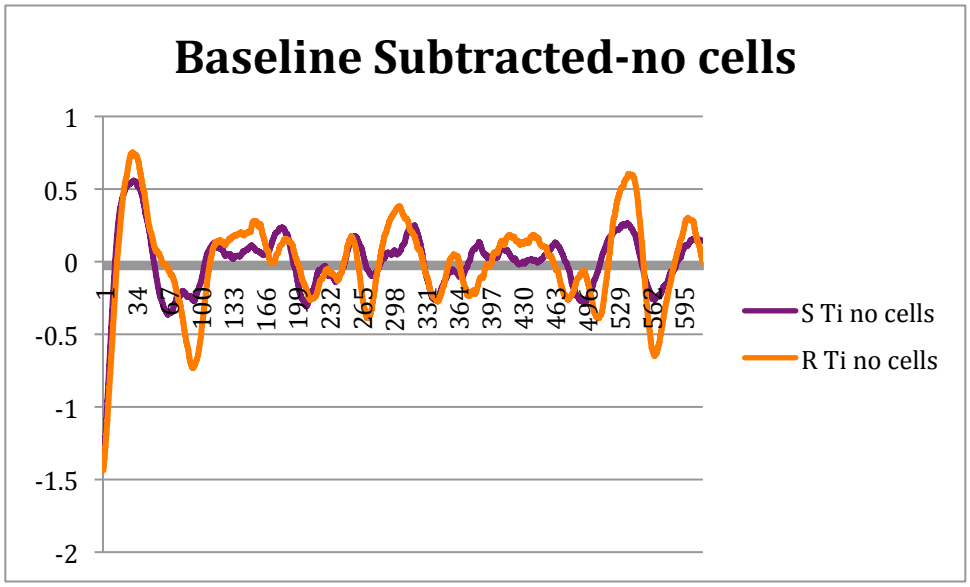

Figure 24. Baseline Subtracted of Titanium with no cells

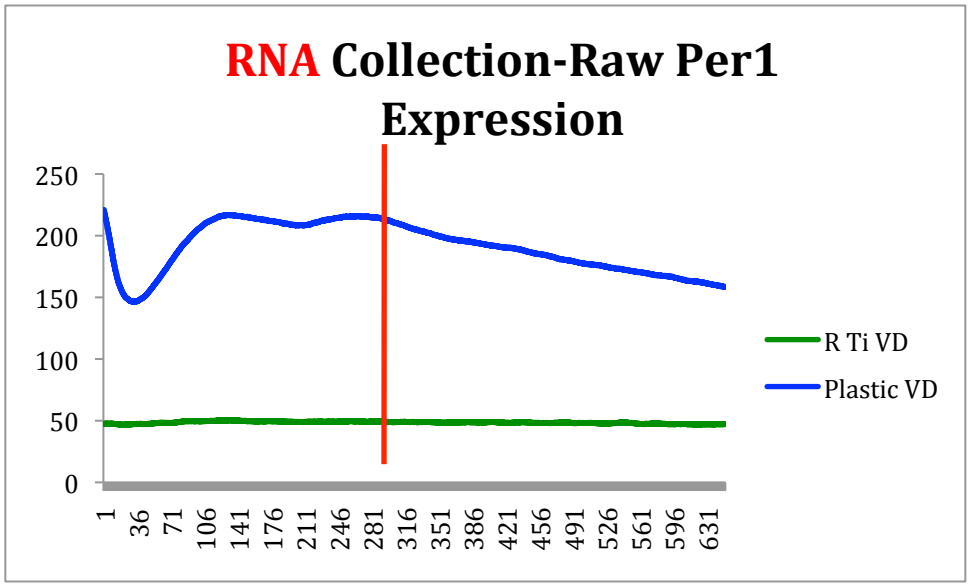

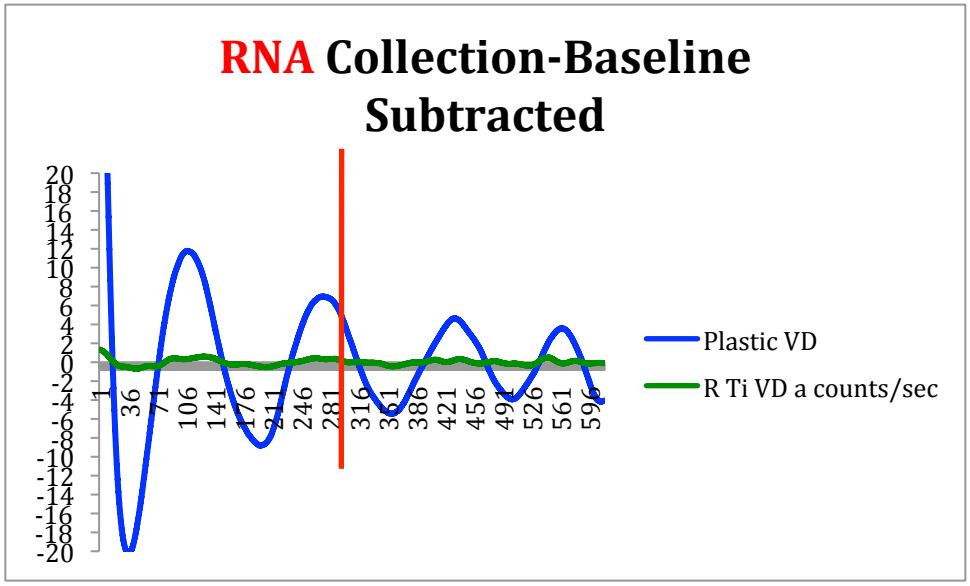

Figure 25. RNA Extraction Time Point

Table. 4 RT-PCR Data

qPCR	Plastic	Plastic	Plastic	R Ti	R Ti	R Ti	Probes	
A	29.343926	28.481087	28.015871	33.863186	32.972786	33.24523	ID2	FAM
B	33.27957	33.847576	33.650158	34.380264	34.63202	34.226948	NPAS2	FAM
C	31.205467	31.468046	31.891237	36.1139	35.57175	35.99598	BMAL1	FAM
D	23.754082	23.484943	23.489176	26.491127	26.444168	25.506884	GAPDH	FAM
E	28.939074	28.944529	29.110989	32.55722	32.183384	32.31696	CLOCK	FAM
F	30.100145	29.942245	29.976044	33.223045	33.48251	33.2521	PER1	FAM
G	33.02766	32.829876	33.217808	37.035255	37.84561	37.622433	PER2	FAM

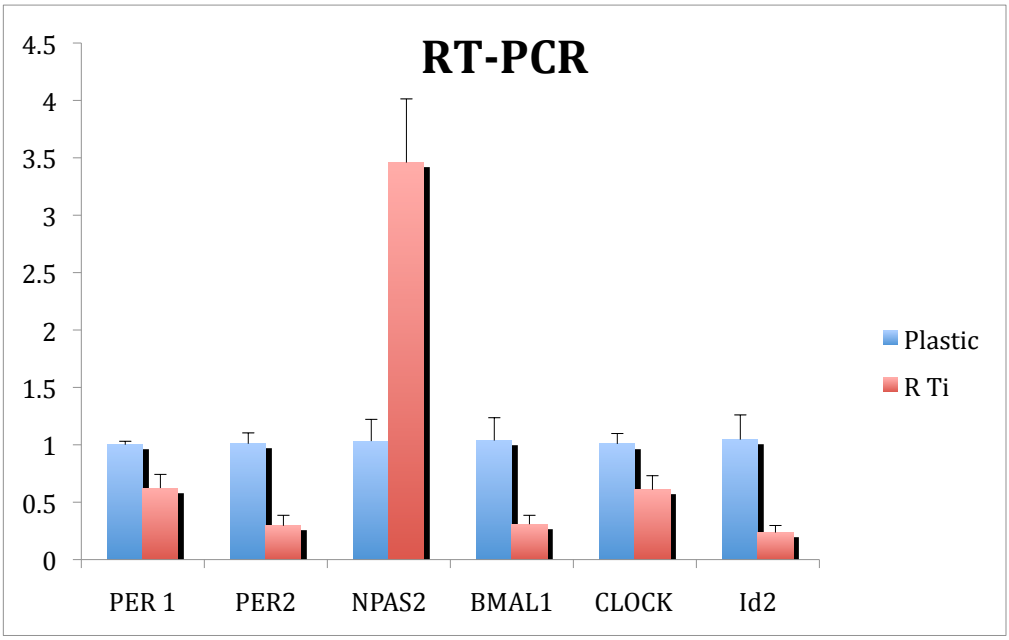

Figure 26. RT-PCR

Table 5. RT-PCR T test

Avg	PER 1	PER2	NPAS2	BMAL1	CLOCK	ID2
Plastic	1.00089022	1.009331646	1.032180138	1.037161773	1.007922107	1.045323173
R Ti	0.623029771	0.294668429	3.45882784	0.308304427	0.608250337	0.235942053
STD Error	PER1	PER2	NPAS2	BMAL1	CLOCK	ID2
Plastic	0.030090447	0.094076384	0.189645154	0.198727519	0.090455166	0.21462844
R Ti	0.119306765	0.091479752	0.554125325	0.077743068	0.122441714	0.061264073
T Test P < 0.05	PER1	PER2	NPAS2	BMAL1	CLOCK	ID2
	0.037257855	0.005520111	0.014337979	0.026889559	0.058464954	0.022233746

Table 6. Diseases Associated with Polymorphism/Deletion of Circadian Rhythm Genes (25)

Disease/disorder	Clock genes	Criteria	References
Studies in humans or human cell lines			
Cancer, various forms	*Per1, Per2*	Tumor mutation, knockdown	[61–63]
	Per1	Decreased expression	[64–66]
	Per1	Growth inhibition by overexpression	[66]
	Per3	Decreased expression	[67]
	Cry2	Polymorphism	[68]
	NPAS2	Polymorphism	[69]
	NPAS2	Mutation, silencing downregulates DNA repair and cell cycle	[70]
Prostate cancer	*Per1, Per2, Per3, Cry1, Cry2, Bmal1, Clk, NPAS2, CsnK1ε*	Polymorphism	[71, 72]
	Per2, Clk	Decreased expression, growth inhibition by *Per2* overexpression	[73]
	Bmal1	Increased expression	[73]
Breast cancer	*Per1, Per2, Per3*	Decreased expression	[74, 75]
	Per1, Per2	Tumor mutation	[62]
	Per2	Knockdown	[76]
	Per3, NPAS2	Polymorphism	[77–79]
	Clk, Cry1	Polymorphism	[80, 81]
	Cry2	Polymorphism	[82]
	Cry2	Silencing suppresses DNA repair	[83]
	NPAS2	Silencing suppresses DNA repair and cell cycle	[70]
Obesity	*Per2*	Polymorphism	[84]
	Clk	Polymorphism	[85–90]
Diabetes type 2	*Cry2*	Polymorphism	[91, 92]
	Bmal1	Polymorphism	[93]
Hypertension	*Bmal1*	Polymorphism	[93]
Major depression	*Cry1, NPAS2*	Polymorphism	[94]
Bipolar disorder	*Cry2*	Decreased expression	[22]
	Per3, Cry2, Bmal1, Bmal2, Clk, Dbp, Tim, CsnK1ε, NR1D1	Polymorphism	[79, 95–101]
Winter depression	*Per2, Cry2, Bmal1, NPAS2*	Polymorphism	[22, 102–104]
Schizophrenia	*Per1*	Decreased expression	[105]
	Per3, Tim, Clk[b]	Polymorphism	[96, 106, 107]
ADHD	*Per1, Clk*	Polymorphism	[108, 109]
Autism	*Per1, NPAS2*	Polymorphism	[110]
Animal models			
Cancer, various forms or cell lines (mouse)	*Per1, Per2,*	Mutations, knockdown, knockout, overexpression	[75, 111–114]
	Per2, Rev-erbα	Targets of tumor suppressors C/EBPα/-ε	[115]
	Per2	Enhanced degradation	[116]
		Tumor suppression by ectopic expression	[117]
Arthritis (mouse)	*Cry1, Cry2*	Knockout	[118]
	Per1, Per2, Bmal1, Dbp	Altered patterns	[118]
Obesity (mouse)	*Per1, Per2, Per3, Cry1, Cry2, Bmal1, Dbp, CsnK1ε, NFIL3*	Altered patterns (liver, kidney)	[119]
	Cry1, Bmal1, Rev-erbα	Decreased expression (brainstem)	[119]
	Clk	Increased expression (brainstem)	[120]
Hypertension (rat)	*Bmal1*	Polymorphism	[93]
Huntington's disease (mouse)	*Cry1, Dbp*	Arrhythmic expression	[28]
	Per2	Phase advance	[28]
Bipolar disorder (mouse)	*Dbp*	Knockout	[121]

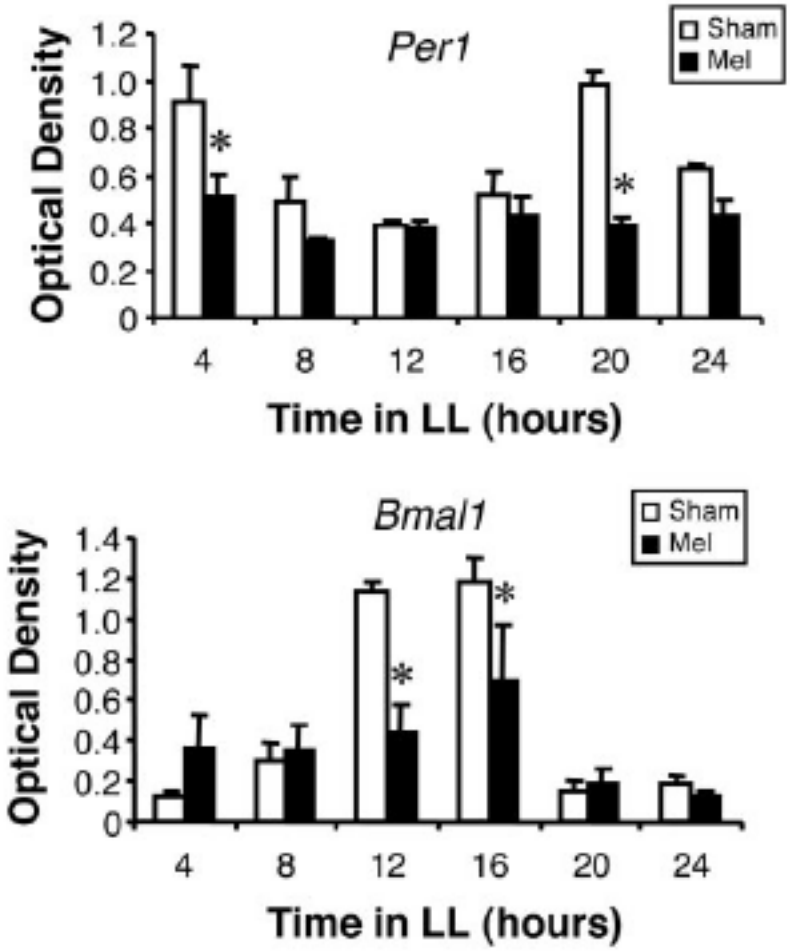

Figure 27. Melatonin Effect of PER1 and BMAL1 (27)

References

1.) Shin Yamazaki, Joseph S. Takahashi. Real-time luminescence reporting of circadian gene expression in mammals. *Methods in Enzymology.* 393:288-301

2.) http://millar.bio.ed.ac.uk/lucifer.html

3.) Kelly, J., Lin, A., Wang, C. J., Park, S., & Nishimura, I. (2009). Vitamin D and bone physiology: Demonstration of vitamin D deficiency in an implant osseointegration rat model. *Journal of Prosthodontics*, *18*(6), 473-478.

4.) Mengatto, C. M., Mussano, F., Honda, Y., Colwell, C. S., & Nishimura, I. (2011). Circadian rhythm and cartilage extracellular matrix genes in osseointegration: a genome-wide screening of implant failure by vitamin D deficiency. *PloS one*, *6*(1), e15848.

5.) Bell-Pedersen, D., Cassone, V. M., Earnest, D. J., Golden, S. S., Hardin, P. E., Thomas, T. L., & Zoran, M. J. (2005). Circadian rhythms from multiple oscillators: lessons from diverse organisms. *Nature Reviews Genetics*, *6*(7), 544-556.

6.) Torres-Farfan, C., Rocco, V., Monso, C., Valenzuela, F. J., Campino, C., Germain, A., ... & Seron-Ferre, M. (2006). Maternal melatonin effects on clock gene expression in a nonhuman primate fetus. *Endocrinology*, *147*(10), 4618-4626.

7.) Filipski, E., King, V. M., Etienne, M. C., Li, X., Claustrat, B., Granda, T. G., ... & Lévi, F. (2004). Persistent twenty-four hour changes in liver and bone marrow despite suprachiasmatic nuclei ablation in mice. *American Journal of Physiology-Regulatory, Integrative and Comparative Physiology*, *287*(4), R844-R851.

8.) http://www.rrrc.us/userfiles/genotyping/09021007RRRC%20Genotypong%20Protocol.pdf

9.) Nathanial Hassan. “Circadian Gene Networks in Bone Regeneration.” (2012)

10.) Rat Resource and Research Center. Room S118, 4011 Discovery Drive, Columbia, MO 65201. http:www.rrrc.us/userfiles/genotyping/09021007RRRC%20273%20Genotyping%20Protocol.pdf

11.) http://www.actimetrics.com/Lumicycle/

12.) L. Le Guehennec, A. Soueidan, P. Layrolle, Y. Amouriq. Surface treatments of titanium dental implants for rapid osseointegration. *Dental Materials* 23 (2007) 844-854.

13.) Wennerberg, Ann, Tomas Albrektsson. On Implant Surfaces: A Review of Current Knowledge and Opinions. *The International Journal of Oral & Maxillofacial Implants* 25.1 (2010): 63.

14.) Mante, M., Daniels, B., Golden, E., Diefenderfer, D., Reilly, G., & Leboy, P. S. (2003). Attachment of human marrow stromal cells to titanium surfaces. *Journal of Oral Implantology*, *29*(2), 66-72.

15.) www.qiagen.com (RNeasy®Mini Handbook) April 2006 1-30 “Animal Cells Spin”

16.) https://cssportal.roche.com/LFR_PublicDocs/…/11644807001_en-12.pdf

17.) Relógio, A., Westermark, P. O., Wallach, T., Schellenberg, K., Kramer, A., & Herzel, H. (2011). Tuning the mammalian circadian clock: robust synergy of two loops. *PLoS computational biology*, *7*(12), e1002309.

18.) Lee, H. M., Chen, R., Kim, H., Etchegaray, J. P., Weaver, D. R., & Lee, C. (2011). The period of the circadian oscillator is primarily determined by the balance between casein kinase 1 and protein phosphatase 1. *Proceedings of the National Academy of Sciences*, *108*(39), 16451-16456.

19.) Reick, M., Garcia, J. A., Dudley, C., & McKnight, S. L. (2001). NPAS2: an analog of clock operative in the mammalian forebrain. *Science*, *293*(5529), 506-509.

20.) Nishimura I, HuangY, Butz F, Ogawa T, Lin L, et al. (2007) Discrete deposition substrate microtopography accelerated osseointegration. Nanotechnology 18:9.

21.) Takahashi JS, Hong HK, Ko CH, McDearmon EL (2008) The genetics of mammalian circadian order and disorder: implications for physiology and disease. Nat Rev Genet 9: 764-775.

22.) DeBruyne, J. P., Weaver, D. R., & Reppert, S. M. (2007). CLOCK and NPAS2 have overlapping roles in the suprachiasmatic circadian clock. *Nature neuroscience*, *10*(5), 543-545.

23). homepage.usask.ca/~ctl271/857/def_homolog.shtm

24.) Dibner, C., Schibler, U., & Albrecht, U. (2010). The mammalian circadian timing system: organization and coordination of central and peripheral clocks. *Annual review of physiology*, *72*, 517-549.

25.) Hardeland, R., Madrid, J. A., Tan, D. X., & Reiter, R. J. (2012). Melatonin, the circadian multioscillator system and health: the need for detailed analyses of peripheral melatonin signaling. *Journal of pineal research*, *52*(2), 139-166.

26.) Tresguerres, I. F., Clemente, C., Blanco, L., Khraisat, A., Tamimi, F., & Tresguerres, J. A. (2012). Effects of local melatonin application on implant osseointegration. *Clinical Implant Dentistry and Related Research*, *14*(3), 395-399.

27). Johnston, J. D., Tournier, B. B., Andersson, H., Masson-Pévet, M., Lincoln, G. A., & Hazlerigg, D. G. (2006). Multiple effects of melatonin on rhythmic clock gene expression in the mammalian pars tuberalis. *Endocrinology*, *147*(2), 959-965.

28). Yi, C., Mu, L., de la Longrais, I. A. R., Sochirca, O., Arisio, R., Yu, H., ... & Katsaro, D. (2010). The circadian gene NPAS2 is a novel prognostic biomarker for breast cancer. *Breast cancer research and treatment*, *120*(3), 663-669.

29. Wu, Y. Y., Yu, T., Yang, X. Y., Li, F., Ma, L., Yang, Y., ... & Gong, P. (2012). Vitamin D< sub> 3</sub> and insulin combined treatment promotes titanium implant osseointegration in diabetes mellitus rats. *Bone*.

30. Dvorak, G., Fügl, A., Watzek, G., Tangl, S., Pokorny, P., & Gruber, R. (2012). Impact of dietary vitamin D on osseointegration in the ovariectomized rat. *Clinical Oral Implants Research*, *23*(11), 1308-1313.

31. www.**clontech**.com/xxclt_ibcGetAttachment.jsp?cItemId=17629